Pressure Management of Drilling Fluid and Study of Overcut Ratio in Horizontal Directional Drilling

by

Bo Gao

A thesis submitted in partial fulfillment of the requirements for the degree of

Master of Science

in
Civil (Cross-Disciplinary)

Department of Civil and Environmental Engineering
University of Alberta

Abstract

Horizontal directional drilling (HDD) has become one of the leading technologies for the installation of underground utilities and other trenchless projects. However, some of the risks associated with HDD, such as hydraulic fracturing and drilling fluid loss, have a considerable impact on construction that may lead to time loss and increased project cost and are major challenges for the industry to overcome. To minimize the risk of hydraulic fracturing and fluid loss, a proper and effective drilling fluid pressure management system is necessary. Moreover, there is still a chance for engineers to develop better design guidelines by optimizing the construction process. During HDD pipe installation, the diameter of the borehole must be larger than the diameter of the product pipe in order to perform a successful pullback operation; and the ratio of borehole diameter to pipe diameter is known as the overcut ratio.

As a result, this thesis is focused on two critical problems in HDD: pressure management and overcut ratio. Accordingly, three major aspects of pressure management of drilling fluid are addressed in this thesis: 1) estimation of maximum allowable and minimum required fluid pressures, 2) modeling of the annular pressure of drilling fluid, and 3) drilling fluid pressure management and monitoring. Maximum allowable prediction methods are categorized based on the approaches used for prediction. The authors also discuss three different rheological models for predicting annular pressure of drilling fluid and provide an overview of drilling fluid pressure management in HDD.

Furthermore, the effect of overcut ratio on the forces acting on steel and polyethylene pipes during HDD pipe installation is discussed in this thesis. To characterize the effect of overcut ratio, total pullback force is assessed in separate components including fluidic drag and change in direction.

Existing methods and standards to calculate total pullback force are investigated. Results indicate that total pullback force decreases with increasing overcut ratio with a higher rate in the case of steel pipes. Change in pullback forces is normalized and quantified as percentages for both steel and Polyethylene (PE) pipes. This approach can be used for a quick and simple evaluation of the total pullback forces when planning HDD. The results indicate an overcut ratio of 1.5 is suitable for steel pipe and an overcut ratio of 1.3 is suitable for PE pipe.

Acknowledgements

I would like to express my sincere gratitude towards my supervisor, Dr. Alireza Bayat, for his continued guidance and support throughout my studies and for providing me with this research opportunity. This research would not be possible without your direction and dedication.

I would also like to thank Dr. Chao Kang, Dr. Leila Hashemian and Dr. Tugce Baser for their guidance and encouragement during my research and for giving me constructive feedback on my research work. I would also like to extend my gratitude to our technical writers, Lindsey Gauthier, Delaina Lawson and Lana Gutwin, for editing and proofreading my thesis.

Finally, I am very grateful for the friends I made during my two years of studies, who brought me joy and support and made my study a wonderful experience. I would also like to express my deepest appreciation to my mom and dad for their encouragement, support and unconditional love.

Table of Contents

List of Tables

List of Figures

List of Symbols and Abbreviations

a: Radius of the cavity during loading

a_0: Radius of the cavity at initial unloaded state

API: American Petroleum Institute

ASTM: American Society for Testing and Materials

c: Cohesion of soil

c_u: Undrained shear strength

d_{bore}: Diameter of borehole

d_{hyd}: Hydraulic diameter

d_p: Pipe external diameter

dp/dz: Energy gradient through the length of the pipe

d_{pipe}: Diameter of drill pipe

DRAG: Fluidic drag between pipe and viscous drilling fluid

E: Young's modulus

f: Fanning friction factor

f_1: Friction coefficient between the pipe and roller-lane or ground surface

f_2: Friction coefficient between pipe and drilling fluid

f_3: Friction coefficient between the pipe and the borehole wall

frict: Friction between pipe and soil

G: Shear modulus

h_{bore}: Height of the mud column

HDD: Horizontal directional drilling

h_s: Depth of borehole below ground surface

h_w: Height of groundwater over the borehole

I: Moment of inertia

ID_{HOLE}: Diameter of hole or inside diameter of casing

k: Consistency index

K_0: Coefficient of the lateral earth pressure at rest

L_{arc}: Length of curved pipe section

L_{bore}: Borehole length

L_k: Lengths of segments of the borehole

n: Flow index

N: Normal contact force between pipe and soil at the center of pipe section

NEN: Netherlands Standardization Organization

OD_{DP}: Outside diameter of the drill pipe or drill collar

OR: Overcut ratio

P: Force from flexural stiffness

P_0: Initial stress of soil

PE: Polyethylene

P_{frac}: Mud pressure at fracture

P_i: Internal mud pressure in the borehole

P_{lim}: Limit cavity pressure

p_{max}: Maximum allowable pressure

P_{min}: Minimum required pressure

PRCI: The Pipeline Research Council International

PV: Plastic viscosity

Q: Weight of the pipe per unit length with fillings

Q_{eff}: Effective weight of the pipe considering the buoyancy force

q_r: Maximum soil reaction near the end of the bend

R: Cavity pressure ratio

R_0: Borehole radius

r_h: Borehole radii

R_{lim}: Limit cavity expansion ratio

r_p: Pipe external radii

$R_{p,max}$: Radius of the plastic zone

RPM: Revolution per minute

T_{id}: Force due to fluidic drag

T_{ig}: Force due to pipe's weight outside the borehole

T_{is}: Force due to pipe's weight inside the borehole

ΔT_{kif}: Sum of all forces resulting from flexural stiffness of a pipe and changes in direction

u: Groundwater pressure

v: Velocity of drilling fluid

v_a: Coefficient of friction applicable at the surface before the pipe enters borehole

V_a: Fluid velocity

v_b: Coefficient of friction applicable within the lubricated borehole or after the (wet) pipe exits

v_p: Pipe velocity

w: Submerged weight of pipe per unit with filled contents

w_a: Weight of empty pipe

w_b: Net upward buoyant force on pipe in borehole

w_p: Weight of the pipe per unit length

YP: Yield point

α: Borehole angle at pipe entry

α_0: Angle between the horizontal and the ground surface in front of the entry point

β: Borehole angle at pipe exit

γ: Shear rate

γ_{mud}: Unit weight of mud

γ: Unit weight of soil above groundwater

γ': Unit weight of soil below groundwater

$\varepsilon_{\theta,max}$: Maximum allowable strain

θ: Angle of the axis of borehole section relative to horizontal line

μ_g: Friction coefficient between the pipe and the ground

μ_{mud}: Fluidic drag coefficient

μ_p: Viscosity of drilling fluid

μ_{soil}: Average frictional coefficient between pipe and soil

ρ_a: Fluid density in the annulus

σ'_0: Initial effective stress

τ: Shear stress

τ_p: Shear stress at the pipe wall due to the fluidic drag

τ_y: Yield point of drilling fluid

υ: Poisson's ratio

φ: Soil friction angle

ψ: Dilation angle of the soil

ψ_0: Half the angle between the two line segments of the borehole

1. Introduction

1.1. Background

Due to the high social and environmental impact of open cut trenching, horizontal directional drilling (HDD) has become increasingly popular for both underground utility and pipeline installations. Developed in the early 1970s, HDD is an effective method for underground construction, especially in difficult circumstances where minimal surface disruption is required, such as busy intersections and congested roads, or where obstacles need to be bypassed, such as river crossings, highways, mountains, and lakes (Kirby et al. 1996; Allouche et al. 2000; Hashash et al. 2011). Compared to open cut construction, HDD often has a lower total project cost (Abdollahipour et al. 2011). HDD consists of three main steps in the construction process: 1) drilling of the pilot hole, 2) reaming of the pilot hole, and 3) pulling back of pipe string (Colwell and Ariaratnam 2003).

1.1.1. Pressure Management

During HDD construction, one of the major concerns is drilling fluid loss. Drilling fluid, also known as drilling mud, consists of mostly bentonite and water with other additives to improve its quality (Lu et al. 2012). Drilling fluid has a significant role in HDD installation process and has various tasks associated with it, which include carrying cuttings out of the borehole and transporting them to the surface, cooling and lubricating the drill pipe and drill bit, stabilizing the borehole, controlling subsurface pressure, providing hydraulic power to the mud motor, and creating buoyant force for the drill pipe and product pipe (Ariaratnam et al. 2007; Shu et al. 2015; Shu and Ma 2015; Vajargah and van Oort 2015). Nonetheless, the loss of drilling fluid could lead to potential problems such as hydraulic fracturing and loss of circulation. In order to minimize

drilling fluid loss, it is critical that a good drilling fluid pressure management system is in place during HDD installation.

There are three important pressures to consider in the drilling fluid pressure management system: the maximum allowable drilling fluid pressure, the minimum required drilling fluid pressure, and the annular pressure of drilling fluid. As a rule of thumb, the annular pressure of drilling fluid should not exceed the maximum allowable drilling fluid pressure and the minimum required drilling fluid pressure should stay above the groundwater pressure (Carlos et al. 2002). Therefore, it is important to obtain an accurate estimation of these three different pressures.

1.1.2. Overcut Ratio

During reaming of the pilot hole, the borehole has to be made large enough so the pipe can be pulled back through the borehole and the ratio of borehole diameter to pipe diameter is called the overcut ratio. Overall, it is concluded that a decrease in overcut ratio will result in an increase in total pullback force (Polak et al., 2004).

Therefore, in order to minimize the total pullback force during HDD installation, the overcut ratio has to be increased. However, an increase in the overcut ratio will cause the pilot hole to be reamed multiple times, which in turn can make the project more costly and time consuming. As a result, an optimal overcut ratio is important for increasing the efficiency of HDD installation projects.

Currently, the industry standard for the overcut ratio is 1.5 times of the pipe diameter (Popelar et al. 1997). Nevertheless, this practice was developed 20 years ago and very little research has been done on the subject. Therefore, it is essential to analyze the role of the overcut ratio in HDD and to provide a theoretical basis of the optimal overcut ratio.

1.2. Objectives

The main objectives of the study are summarized as follows:

- To perform a comprehensive literature review on methods available to estimate the maximum and minimum required drilling fluid pressures
- To provide an overview of pressure management in HDD
- To compare annular drilling fluid pressure loss using different rheological models
- To analyze the difference in the overcut ratio for steel and PE
- To investigate the role of overcut ratio and to find a theoretical value of overcut ratio that is the most appropriate for HDD installation
- To develop a reference for a fast and simple estimation of total pullback force using different overcut ratio

1.3. Methodology

Based on literature review, four different analytical approaches for estimating maximum allowable drilling fluid pressure, the Delft equation (Delft Geotechnics 1997), maximum strain solution (Verruijt 1993), the Queen's equation (Xia and Moore 2006), and the Yu and Houlsby equation (1991) are discussed and compared; empirical approach, experiments and numerical analysis for estimating maximum allowable drilling fluid pressure are also examined. Additionally, three different rheological models, Bingham Plastic model (1922); Power Law model (Blair et al. 1939), and Herschel–Bulkley model (1926) are used for predicting annular drilling fluid pressure loss. A case study is performed to compare the annular drilling fluid pressure loss for the three rheological models.

Based on literature review, four different methods, PRCI method (1996), ASTM F1962 method (2011), NEN 3650 method (2007) and Pipeforce method (2007) are used for calculating total pullback force in HDD installation. A case study is carried out to compare these four different methods for steel and PE pipes. Furthermore, different force components in the Pipeforce method

are analyzed and compared for different overcut ratios and pipe diameters. In the end, normalization curves of total pullback force with respect to the overcut ratio for steel and PE pipes are plotted.

1.4. Thesis Structure

This thesis is organized as the following:

- Chapter 1 – Introduction: In this chapter, a brief background on HDD, the importance of pressure management and overcut ratio are presented. The thesis objectives, thesis methodology, and thesis structure are also discussed.

- Chapter 2 – Literature Review: In this chapter, a detailed literature review on methods for estimating maximum allowable pressure, a method for estimating minimum required pressure and methods for estimating total pullback force is presented.

- Chapter 3 – Study of Pressure Management in Horizontal Directional Drilling: In this chapter, the maximum allowable pressure in HDD is analyzed using four different approaches: analytical approaches, empirical approach, experiments and numerical simulation. Three different rheological models of drilling fluid are used to predict annular pressure loss of drilling fluid. A case study is used to verify the models. In the end, the general procedure of pressure management in HDD is given.

- Chapter 4 – Analysis of the Role of Overcut Ratio in Horizontal Directional Drilling: In this chapter, four different methods for estimating total pullback force are analyzed and discussed, and a case study is presented to compare the four different methods. Pipeforce method is used to examine the effect of overcut ratio in HDD for both steel and PE pipes. Two case studies are presented to verify the suggested model.

- Chapter 5 – Conclusions: In this chapter, the thesis is summarized and its major findings are reviewed. Moreover, suggested future research is outlined.

2. Literature Review

2.1. Methods for Estimating Maximum Allowable Pressure

Maximum allowable drilling fluid pressure is defined as the maximum pressure soil can sustain without failure (Staheli et al. 2010) and the methods for estimating maximum allowable pressure are often derived from mathematical models and theories, and presented as analytical solutions. In this chapter, four different analytical methods, the Delft equation (Delft Geotechnics 1997), maximum strain solution (Verruijt 1993), the Queen's equation (Xia and Moore 2006), and the Yu and Houlsby equation (1991) are reviewed.

2.1.1. The Delft Equation

The Delft equation is based on cavity expansion theory, and was originally proposed by Vesic (1972), and Luger and Hergarden (1988) applied the solution to HDD. The theory is largely based on the Mohr-Coulomb failure criterion and Hooke's Law. As the borehole is being drilled, pressure from the drilling fluid and other sources is exerted on the wall of the borehole. The pressure on the wall gradually increases as it reaches the maximum pressure, which is the Mohr-Coulomb onset yield stress. As more and more pressure is exerted on the wall of the borehole, the borehole diameter also increases elastically. The maximum allowable pressure is measured at the largest radial displacement, or when plastic expansion occurs (e.g. Staheli et al. 1998; Rostami et al. 2016). The pressure expansion in the borehole is given in Figure 2-1.

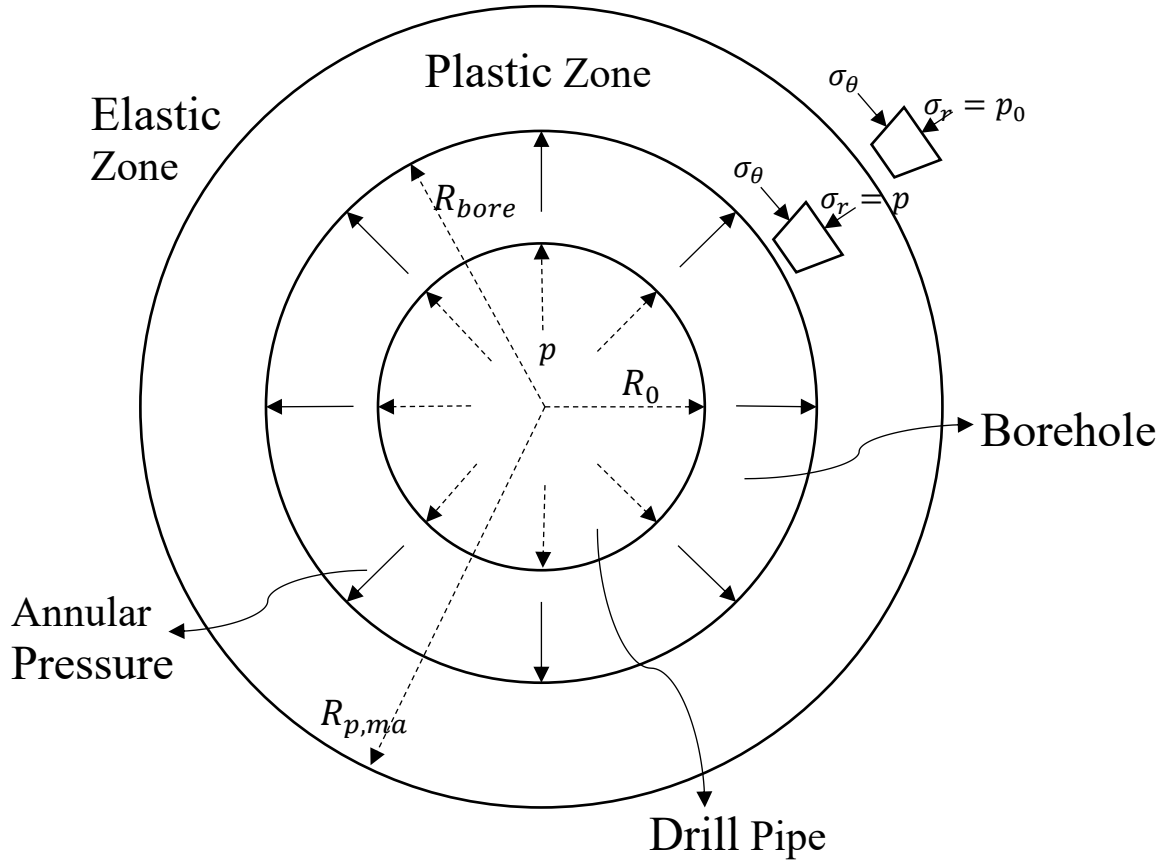

Figure 2-1. Pressure expansion in borehole (after Rostami et al. 2016)

The Delft equation considers both the soil friction angle and the cohesion angle with some assumptions. Major assumptions associated with the approach are as follows: the borehole is assumed to be axi-symmetric; the soil medium is isotropic, homogeneous and have infinite size; stress response is elastic until onset failure as defined by the Mohr-Coulomb failure criterion; elastic deformation is governed by Hooke's law; volume change in the plastic zone is zero and the elastic deformation in the plastic zone is neglected; and stress in soil medium is independent of gravity and in isotropic stress condition (e.g., Xia 2006; Rostami et al. 2016). The maximum allowable pressure in the Delft equation can be calculated as follows:

$$p_{\max} = u + \left[\sigma'_0\left(1+\sin\varphi\right) + c\cos\varphi + c\cot\varphi\right]\cdot\left(\left(\frac{R_0}{R_{p,\max}}\right)^2 + \frac{\sigma'_0\sin\varphi + c\cos\varphi}{G}\right)^{\frac{-\sin\varphi}{1+\sin\varphi}} - c\cdot\cot\varphi \qquad [1]$$

where p_{max} is maximum allowable pressure (Pa), u is groundwater pressure (Pa), φ is soil friction angle (°), c is cohesion of soil (Pa), R_0 is borehole radius (m), $R_{p,max}$ is radius of the plastic zone (m), G is shear modulus (Pa), and σ'_0 is initial effective stress (Pa). σ'_0 is calculated as follows:

$$\sigma'_0 = \gamma\cdot\left(h_s - h_w\right) + \gamma'\cdot h_w \qquad [2]$$

where γ is unit weight of soil above groundwater (N/m^3), γ' is unit weight of soil below groundwater (N/m^3), h_s is the depth of borehole below ground surface (m), and h_w is the height of groundwater over the borehole (m). For purely cohesive soil, the radius of the plastic zone should be selected as half of the depth of the borehole from the crown to the ground surface ($R_{p,max}$=0.5h). The radius of the plastic zone should be two-thirds of the cover of depth ($R_{p,max}$=2h/3) for non-cohesive soils (Van and Hergarden, 1997; Xia 2006).

2.1.2. Maximum Strain Solution

Maximum strain solution is another alternative that utilizes the cavity expansion theory to calculate the maximum allowable pressure in the borehole and was developed by Verruijt (1993). Compared to the Delft solution, this method uses maximum hoop strain around the borehole instead of the Mohr-Coulomb failure criterion (plastic region) and Hooke's Law (elastic region). However, the mechanics of both the Delft solution and the maximum strain solution are essentially the same. If the strain around the borehole exceeds its upper limits, mud is pushed aside and cracks form. Thus, drilling fluid may escape from the cracks and cause hydraulic fracturing. By assuming a maximum

allowable strain for a borehole, maximum allowable pressure can be calculated as follows (Keulen 2001):

$$P_{\max} = \left\{ \left[\varepsilon_{\theta,\max} \times \frac{2G}{P_0 + c \cdot \cot\varphi} \times \frac{1+m}{1-m} \right]^{\frac{1-m}{1+k}} \times \frac{2}{1+m} \left(P_0 + c \cdot \cot\varphi \right) \right\} - c \cdot \cot\varphi \quad [3]$$

where $\varepsilon_{\theta,max}$ is the maximum allowable strain, P_0 is initial stress of soil (Pa), ψ is the dilation angle of the soil (°), m=(1-sinφ/1+sinφ), and k=(1-sinψ/1+sinψ). When the dilation angle ψ=0, k becomes 1 accordingly and Eq. 3 becomes as follows:

$$P_{\max} = \left(\left(\frac{R_{p,\max}}{R_0} \right)^{\frac{2\sin\varphi}{1+\sin\varphi}} \cdot \left(1+\sin\varphi\right) \cdot \left(\sigma'_0 + c \cdot \cot\varphi \right) \right) - c \cdot \cot\varphi \quad [4]$$

The complete derivation can be found in Keulen (2001). Different from the Delft solution, maximum strain method utilizes strain instead of stress as a deciding factor. More importantly, it incorporates the dilation angle into the equation.

2.1.3. Queen's Equation

The Queen's equation was first introduced by Xia and Moore (2006) as an improvement to both the Delft solution and the solution proposed by Kennedy et al. (2004a, b). Equations by Kennedy et al. (2004a, b) are given as follows:

$$P_{frac} = \left(3K_0 - 1\right)P_0 \text{ for } K_0 \langle 1 \quad [5a]$$

$$P_{frac} = \left(3 - K_0\right)P_0 \text{ for } K_0 \rangle 1 \quad [5b]$$

where P_{frac} is the pressure at fracture (Pa) and K_0 is the coefficient of the lateral earth pressure at rest. A solution provided by Kennedy et al. (2004a, b) is based on finite-element analysis to test soils under different pressures and elastic continuum theory. From the test results, it was observed that tensile fractures occurred at the crown of the borehole ($K_0 < 1$) and the spring-line ($K_0 > 1$). According to Xia and Moore (2006), the Delft solution overestimates the critical mud pressure for the lower values of coefficient of lateral earth pressure at rest ($K_0 < 0.85$) and the solution proposed by Kennedy et al. (2004b) does not account for all values of K_0. Therefore, for a more accurate estimation of the maximum allowable pressure, the Queen's equation was developed to correct the flaws in both the Delft solution and the solution provided by Kennedy et al. (2004).

The Queen's equation examines the growth of maximum plastic radius with increasing mud pressure and applies two scenarios: one is when the maximum plastic radius appears at the crown of the borehole ($K_0 < 1$), and the other is when the maximum plastic radius appears at the spring-line ($K_0 > 1$). The Queen's equation was developed using cavity expansion theory and takes the effects of the coefficient of lateral earth pressure at rest into consideration. In addition, based on Xia and Moore's research, there are three assumptions for the Queen's equation: the borehole has an axisymmetric plastic zone, the displacement of each point on the interface between plastic and elastic zone is consistent, and the displacement is closely related to the radius of the maximum plastic zone (Xia and Moore 2006). The Queen's equation is expressed as follows:

$$P_i = c_u + 0.5(3K_0 - 1)P_0 - c_u \ln\left(\left(\frac{R_0}{R_{p,\max}}\right)^2 + \left(\frac{c_u + 1.5(K_0 - 1)P_0}{G}\right)\right), K_0 \langle 1 \qquad [6a]$$

$$P_i = c_u + 0.5(3 - K_0)P_0 - c_u \ln\left(\left(\frac{R_0}{R_{p,\max}}\right)^2 + \left(\frac{c_u + 1.5(1 - K_0)P_0}{G}\right)\right), K_0 \rangle 1 \qquad [6b]$$

where P_i is internal mud pressure in the borehole (Pa) and c_u is the undrained shear strength (Pa). As stated in Xia and Moore (2006), the biggest difference between the Delft solution and the Queen's equation is the incorporation of the coefficient of lateral earth pressure at rest. The Delft solution assumes that K_0 is equal to 1. However, in field conditions, K_0 is not always 1. For instance, K_0 ranges from 0.35 to 0.65 for sand and may be more than 3 for heavily over-consolidated clay (Mesri and Hayat 1993). For K_0 of 1, the Queen's equation produces similar results to the Delft equation. Nevertheless, since the Queen's equation is a newly developed method, all the calculations are based purely on simulation and theory. More field data and experiments are needed to prove that it is the better solution.

2.1.4. Yu And Houlsby Solution

The Yu and Houlsby solution was proposed by Yu and Houlsby (1991) to represent the cavity expansion theory in frictional-cohesive soil. The solution describes the distribution of stress and displacement fields of soil as the pressure builds up to the limiting pressure. Yu and Houlsby's method assumes that the soil is isotropic and elastic-perfectly plastic. The solution obeys Hooke's Law for elastic deformation and uses Mohr-Coulomb failure criterion for onset of yield with a non-associated flow rule. For large strain in the plastic zone, an explicit expression for the pressure expansion relation is derived by integrating the governing equation with the aid of a series expansion as follows:

$$\frac{a}{a_0} = \left(\frac{R^{-\gamma}}{(1-\delta)^{(\beta+m)/\beta} - \left(\frac{\gamma}{\chi}\right)\Lambda_1(R,\xi)} \right)^{\beta/(\beta+m)} \quad [7]$$

According to Eq. 7, as the radius of the cavity approaches infinity, the limiting pressure can be attained (Carter et al. 1986). Thus, the ratio of a/a_0 approaches infinity and the limiting pressure can be obtained using the following equations:

$$\Lambda_1(R_{\lim},\xi) = \frac{\chi}{\gamma}(1-\delta)^{(\beta+m)/\beta} \quad [8]$$

$$R_{\lim} = \frac{(m+a)[Y+(a-1)P_{\lim}]}{a(1+m)[Y+(a-1)P_0]} \quad [9]$$

where a is the radius of the cavity during loading; a_0 is the radius of the cavity at initial unloaded state; R is the cavity pressure ratio; P_{lim} is the limit cavity pressure; m is the indicator for cylindrical analysis where m is equal to 1 and spherical analysis where m is equal to 2; R_{lim} is the limit cavity expansion ratio; υ is the poisson's ratio; ξ, χ, γ, and δ are the material function properties; α is the function of the friction angle; β is the function of the dilation angle; and Y is the function of the cohesion and the friction angle. However, the solution provided by Yu and Houlsby (1991) is more complicated and sophisticated than the other methods described above. Simple hand calculations are not feasible for this method as there is an infinite series involved in the calculation, and a software algorithm is required to find the solution with multiple iterations (Elwood 2008). Elwood (2008) also discusses that the Yu and Houlsby solution overestimates the maximum allowable pressure when compared with both experimental and numerical solutions based on the finite

element method. Similarly, calculations carried out by Rostami (2016) also confirmed Elwood's findings.

Moreover, Mo and Yu (2016) have developed a new method for calculating limit cavity pressure that is based on the quasi-static equilibrium equation for cavity expansion. This method assumes that soil close to the cavity is in critical condition and states that the limit cavity pressure can be reached by considering the plastic zone around the borehole as the critical state region. However, this method is only recently established, and more research is required to gain a better understanding.

2.2. Method for Estimating Minimum Required Pressure

The minimum required pressure is the pressure that must be maintained to prevent a collapsed borehole and that the drilling fluid must overcome in order for it to flow in the borehole (Carlos et al. 2002). There are several negative consequences caused by a collapsed borehole, such as creating high friction on the drill pipes or the product pipe, which may cause damage to the pipes or reduce the service life due to the high-tension stress (Xia 2009). To maintain the stability of a borehole, a minimum required pressure must be applied that is greater than the pore water pressure acting in the soil. In comparison to the maximum allowable pressure, the estimation of minimum required pressure is more straightforward as it is only a threshold pressure for the drilling fluid to start or maintain flowing. Generally, the minimum required pressure for drilling fluid to start flowing can be estimated using the mud weight (Carlos et al. 2002) and it is calculated as follows:

$$P_{\min} = h\gamma_{mud} \qquad [10]$$

where P_{min} is the minimum required pressure (Pa), h is the difference in elevation between the bore and the exit point of the mud flow (m), and γ_{mud} is the unit weight of mud (N/m^3).

The minimum required pressure is dependent on multiple variables, such as the drilling fluid weight, drilling fluid velocity, diameter of the borehole, length of the borehole, and the cover of depth. For a more accurate estimation of the minimum required pressure to maintain drilling fluid flowing, the equation proposed by (Bennett and Wallin 2008) can be used as follows:

$$P_{\min} = \left[\frac{7.48\gamma_{mud} h_{bore}}{144} + L_{bore} \left(\frac{\mu_p \upsilon}{1000\left(d_{bore} - d_{pipe}\right)^2} + \frac{\tau_y}{200\left(d_{bore} - d_{pipe}\right)} \right) \right] \quad [11]$$

where h_{bore} is the height of the mud column (ft), L_{bore} is the borehole length (ft), μ_p is viscosity of drilling fluid (cp), v is the velocity of drilling fluid (ft/s), d_{bore} is the diameter of borehole (in.), d_{pipe} is the diameter of drill pipe (in.), and τ_y is yield point of drilling fluid (lb/100ft^2). Baumert et al. (2005) reported that the use of Eq. 10 results in an overly conservative estimation if a laminar flow value for yield point is used since a laminar flow has a higher yield point than turbulent flow. Therefore, Baumert et al. (2005) suggest using a turbulent flow value yield point, which has a lower value yield point compared to laminar flow, for the above equation to obtain a more accurate estimation (Bennett and Wallin 2008).

2.3. Methods for Estimating Total Pullback Force

Total pullback force is defined as the tensile load that is applied to the pipe during the pullback stage of HDD installation and overcut ratio plays a major role in it. Therefore, in order to properly evaluate the effect of overcut ratio on total pullback force, four methods that are used to predicting total pullback force, PRCI method (1996), ASTM F1962 method (2011), NEN 3650 method (2007) and Pipeforce method (2007) are reviewed.

2.3.1. PRCI Method

PRCI method is developed by Huey et al. (1996) to estimate the total pullback force during HDD installation and is primarily used for steel installation. The calculation of total pullback force is

divided into two parts: total pullback force in straight pipe section and total pullback force in curved pipe section. The straight pipe sections are defined as those with a zero borehole curvature or with a very slight curvature; and the curved sections are assumed to have a constant radius of curvature for the entire section. The drill path for this method can be divided into as many sections as desired; however, the straight pipe sections should remain as long as possible. Moreover, it is assumed that all sections should have continuous connections and are completely free of external moment (Huey et al. 1996).

Another assumption for this method is that the maximum pullback force occurs when the pipe surfaces from the pipe entry point. Axial loads during pullback process are distributed along the straight and curved sections from pipe entry to pipe exit point; the sum of all the individual forces of different sections at the end of pullback process is the total pullback force (Cai et al. 2017). However, PRCI method does not consider the effect of friction when the pipe is outside the borehole, this may cause the total pullback force to be underestimated (Yan et al. 2018).

The following equations are used to calculate total pullback force for straight sections:

$$T_2 = T_1 + |\, frict^1 \,| + DRAG \pm wL\sin\theta \quad [12]$$

$$frict^1 = wL\cos\theta\mu_{soil} \quad [13]$$

$$DRAG = \pi DL\mu_{mud} \quad [14]$$

where T_2 is the tension applied at the left end of pipe section required to overcome friction and drag forces (N); T_1 is the tension applied at the right end of pipe section (N); *frict* is the friction between pipe and soil (N); *DRAG* is the fluidic drag between pipe and viscous drilling fluid (N); *w* is the submerged weight of pipe per unit with filled contents (N/m); L is the length of pipe section (m); θ is the angle of the axis of borehole section relative to horizontal line (rad); μ_{soil} is the average frictional coefficient between pipe and soil, recommended values between 0.21 and

0.30; D is the outside diameter of pipe (m); μ_{mud} is the fluidic drag coefficient, recommended value 345 Pa (0.05 psi).

The following equations are used to calculate total pullback force for curved sections:

$$T_2 = T_1 + 2\times|\ frict^2\ | + DRAG \pm wL_{arc}\sin\theta \quad [15]$$

$$frict^2 = N\mu_{soil} \quad [16]$$

where L_{arc} is the length of curved pipe section (m); N is the normal contact force between pipe and soil at the center of pipe section (N).

The ± term of Equation [12] is defined as (-) if the direction of T_2 is downhole; (+) if the direction of T_2 is upslope and (0) if the pipe section is horizontal. Moreover, the term N is determined by a three-point bending beam model and an iterative calculation is required to obtain the value of N. For more information on PRCI method, please refer to the work done by Huey et al. (1996).

2.3.2. ASTM F1962 Method

The ASTM F1962 method is established by American Society for Testing and Materials in 2011 for estimating the total pullback force in PE pipes. The force due to pullback is calculated at four different transition point A, B, C and D as shown in Figure 2-2, where the total pullback force can be calculated at point D. This method is based on assumptions that there is no collapse and cutting in the borehole, the bending curvature is constant and gradual and the drilling fluid has a relatively low viscosity. However, ASTM F1962 method does not account for the resistance due to the pipe stiffness at bending curves. As a result, a small bending radius and low overcut ratio will greatly affect the final outcome. To combat this effect, larger bending radius and greater overcut ratio are suggested for using this method (ASTM F1962 2011). For borehole geometry, it is assumed that the entry and exit points of the borehole have the same elevation and the middle section of the borehole is horizontal (Yan et al. 2018). Based on the assumptions mentioned above, the total

pullback force for ASTM F1962 method consists primarily of four different components: the friction between pipe and ground, the friction between pipe and borehole, fluidic drag friction and the friction due to capstan effect.

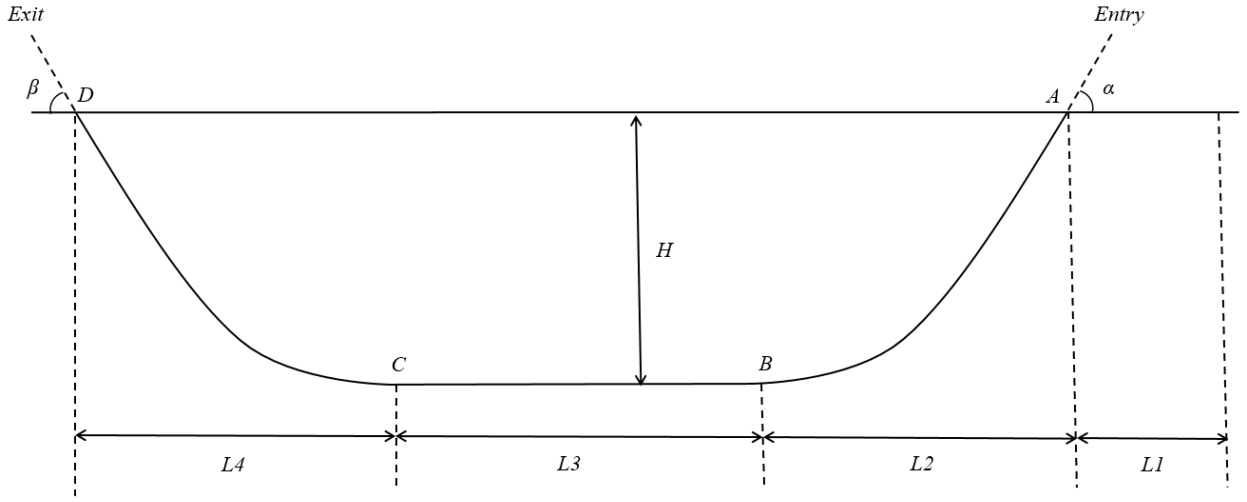

Figure 2-2. Borehole profile for ASTM F1962 method

The following equations are used to calculate total pullback force for ASTM F1962 method:

$$T_A = \exp(v_a\alpha)(v_a w_a (L_1 + L_2 + L_3 + L_4)) \quad [17]$$

$$T_B = \exp(v_b\alpha)(T_A + v_b \mid w_b \mid L_2 + w_b H - v_a w_a L_2 \exp(v_a\alpha)) \quad [18]$$

$$T_C = T_B + v_b \mid w_b \mid L_3 - \exp(v_b\alpha)(v_a w_a L_3 \exp(v_a\alpha)) \quad [19]$$

$$T_D = \exp(v_b\beta)(T_C + v_b \mid w_b \mid L_4 - w_b H - \exp(v_b\alpha)(v_a w_a L_4 \exp(v_a\alpha))) \quad [20]$$

where T_A is the pull force on pipe at point A (N); T_B is the pull force on pipe at point B (N); T_C is the pull force on pipe at point C (N); T_D is the pull force on pipe at point D (N); L_1 is the additional length of pipe required for handling and thermal contraction (m); L_2 is the horizontal distance to achieve desired depth (m); L_3 is the additional distance traversed at desired depth (m); L_4 is the horizontal distance to rise to surface (m); H is the depth of borehole from ground surface (m); v_a is the coefficient of friction applicable at the surface before the pipe enters borehole; v_b is the

coefficient of friction applicable within the lubricated borehole or after the (wet) pipe exits; w_a is the weight of empty pipe (N/m); w_b is the net upward buoyant force on pipe in borehole (N/m); α is the borehole angle at pipe entry (rad); and β is the borehole angle at pipe exit (rad).

2.3.3. NEN 3650 Method

NEN 3650 method is proposed by Netherlands Standardization Organization (NEN) as a means to calculate total pullback force in HDD (2007). The total pullback force for this method is divided into five different components: force due to friction between pipe and roller (T_1); force due to friction in straight section of pipe (T_2); force due to friction in curved section of pipe (T_{3a}); force due to soil reaction in curved section of pipe (T_{3b}) and friction due to curved forces (T_{3c}). The sum of those five forces is the total pullback force (D-Geo Pipeline User Manual 2016). Forces due to friction in straight and curved section of pipe are consist of force due to friction between pipe and borehole and fluidic drag force; and forces due to friction from pipe stiffness at bending and friction from Capstan Effect are accounted for in T_{3b} and T_{3c} respectively.

The series of equations that describe NEN 3650 method are listed below:

$$T_{total} = T_1 + T_2 + T_{3a} + T_{3b} + T_{3c} \quad [21]$$

$$T_1 = f_{install} \times L_{roller} \times Q \times f_1 \quad [22]$$

$$T_2 = f_{install} \times L_2 \times (\pi D_0 \times f_2 + Q_{eff} \times f_3) \quad [23]$$

$$T_{3a} = f_{install} \times L_{arc} \times (\pi D_0 \times f_2 + Q_{eff} \times f_3) \quad [24]$$

$$T_{3b} = f_{install} \times 2 \times q_r \times D_0 \times \frac{\pi}{\lambda} \times f_3 \quad [25]$$

$$T_{3c} = f_{install} \times L_{arc} \times g_t \times f_3 \quad [26]$$

where $f_{install}$ is load factor for normal crossing cases (1.4) and for cases with gravel layer (2.0); L_{roller} is the length of the pipe on the roller-lane or ground surface (m); Q is the weight of the pipe

per unit length with fillings (N/m); f_1 is the friction coefficient between the pipe and roller-lane or ground surface, 0.3 is recommended while 0.1 is used when the roller system is adopted; L_2 is the length of pipe in straight section of borehole (m); D_0 is the outside diameter of the pipe (m); f_2 is the friction coefficient between pipe and drilling fluid, 50 Pa is suggested; Q_{eff} is the effective weight of the pipe considering the buoyancy force (N/m); f_3 is the friction coefficient between the pipe and the borehole wall, recommended value is 0.2; L_{arc} is the length of the bend (m); q_r is the maximum soil reaction near the end of the bend (N/m^2); g_t is the curved force (N/m).

2.3.4. Pipeforce Method

The Pipeforce method is proposed by Cheng and Polak in 2007 and is based on the following assumptions: 1) the bore path is composed of straight sections with defined angles of inclination and is connected by a series of nodes as shown in Figure 2-3; 2) soil around the borehole is considered as a stiff support for the pipe, which means that there is no collapse in the borehole; 3) the pipe must bend around the corner (node) and follow the geometry of the borehole; 4) the geometry of the pipe around corner (node) is modeled as a combination of scenarios, there are five types of scenarios for a total of sixteen different combinations for the geometry of the node; 5) the pipe segment around corner point is considered to be in equilibrium and 6) laminar flow of Newtonian fluid is used in the calculation of fluidic drag friction (Cheng and Polak 2007, Royal et al. 2010, Cai et al. 2017).

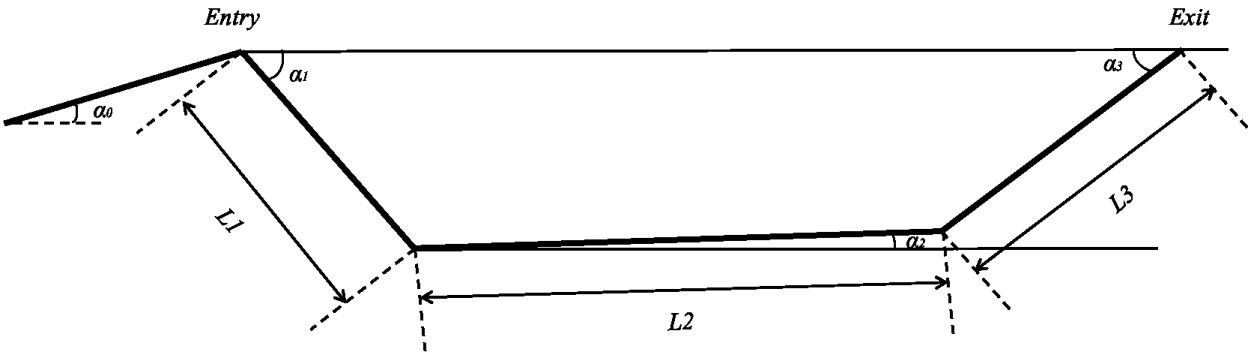

Figure 2-3. Borehole profile for Pipeforce method

However, there are certain limitations associated with the assumptions above. The bore path is consist of straight line segment connected by nodes, thus the pipe angle created by such assumption will be larger than the pipe angle in a real HDD installation (Polak and Chu 2005). Moreover, soil is assumed as rigid throughout the borehole, the borehole will not deflect and will retain its shape. This will cause the friction due to change of direction to be overestimated (Cai et al. 2017).

The total pullback force for Pipeforce method is divided into four different components: force due to friction between pipe and soil, force due to friction between pipe and borehole, force due to fluidic drag friction and force due to bending stiffness and change of direction (Polak and Chu 2005). The equation below describes the total pullback force:

$$T_i = T_{ig} + T_{is} + T_{id} + \sum_{k=1}^{i-1} \Delta T_{kif} \quad [27]$$

where T_{ig} is the force due to pipe's weight outside the borehole (N); T_{is} is the force due to pipe's weight inside the borehole (N); T_{id} is the force due to fluidic drag (N); and ΔT_{kif} is the sum of all forces resulting from flexural stiffness of a pipe and changes in direction (N).

Force due to friction between pipe and soil is described as below:

$$T_{ig} = (w_p \mu_g \cos\alpha_0 + w_p \sin\alpha_0)(L - \sum_{k=0}^{i-1} L_k) \quad [28]$$

where w_p is the weight of the pipe per unit length (N/m); μ_g is the friction coefficient between the pipe and the ground; L is the total length of the pipe (m); L_k is the lengths of segments of the borehole (m); and α_0 is the angle between the horizontal and the ground surface in front of the entry point (rad).

Force due to friction between pipe and borehole is described as below:

$$T_{is} = \sum_{k=0}^{i-1} (| L_k w \mu_b \cos\alpha_k | + L_k w \sin\alpha_k) \quad [29]$$

where w is the submerged weight of the pipe per unit length (N/m); μ_b is the friction coefficient between the pipe and the borehole; and α_k is the angle between the horizontal and the segment k (rad).

The following equations depict force due to fluidic drag:

$$T_{id} = \sum_{k=0}^{i-1} f_d L_k \quad [30]$$

$$f_d = K \times \pi d_p \tau_p \quad [31]$$

where τ_p is the shear stress at the pipe wall due to the fluidic drag (N/m^2); d_p is the pipe external diameter (m); and K is a parameter, which accounts for approximations of the fluidic model, recommended value is 10.

The shear stress at the pipe wall and energy gradient can be calculated as follow:

$$\tau_p = \frac{1}{4}\frac{dp}{dz}\left(2r_p - \frac{r_p^2 - r_h^2}{\ln(\frac{r_p}{r_h})}\frac{1}{r_p}\right) + \frac{\mu \upsilon_p}{\ln(\frac{r_p}{r_h})}\frac{1}{r_p} \quad [32]$$

$$Q = \frac{\pi}{8\mu}\frac{dp}{dz}\left(r_p^4 - r_h^4 - \frac{(r_p^2 - r_h^2)^2}{\ln(\frac{r_p}{r_h})}\right) + \frac{\pi}{2}\frac{\upsilon_p}{\ln(\frac{r_p}{r_h})} \times (r_p^2 - r_h^2 - 2r_p^2 \ln(\frac{r_p}{r_h})) \quad [33]$$

where μ is the viscosity of the fluid (N s/m^2); dp/dz is the energy gradient through the length of the pipe (N/m^3); v_p is the pipe velocity (m/s); r_p is the pipe external radii (m) and r_h is the borehole radii (m).

Based on the borehole and pipe geometry as shown in Figure 2-4, the following equations can be derived:

$$l = c^{'} / (\tan\psi_0 - y_{\max} / l) \quad [34]$$

$$c^{'} = \frac{d_p + c}{\cos\psi_0} - d_p \quad [35]$$

where c is the clearance between the pipe and the borehole (m); ψ_0 is the half the angle between the two line segments of the borehole (rad); and l is the half of the distance between supports (m).

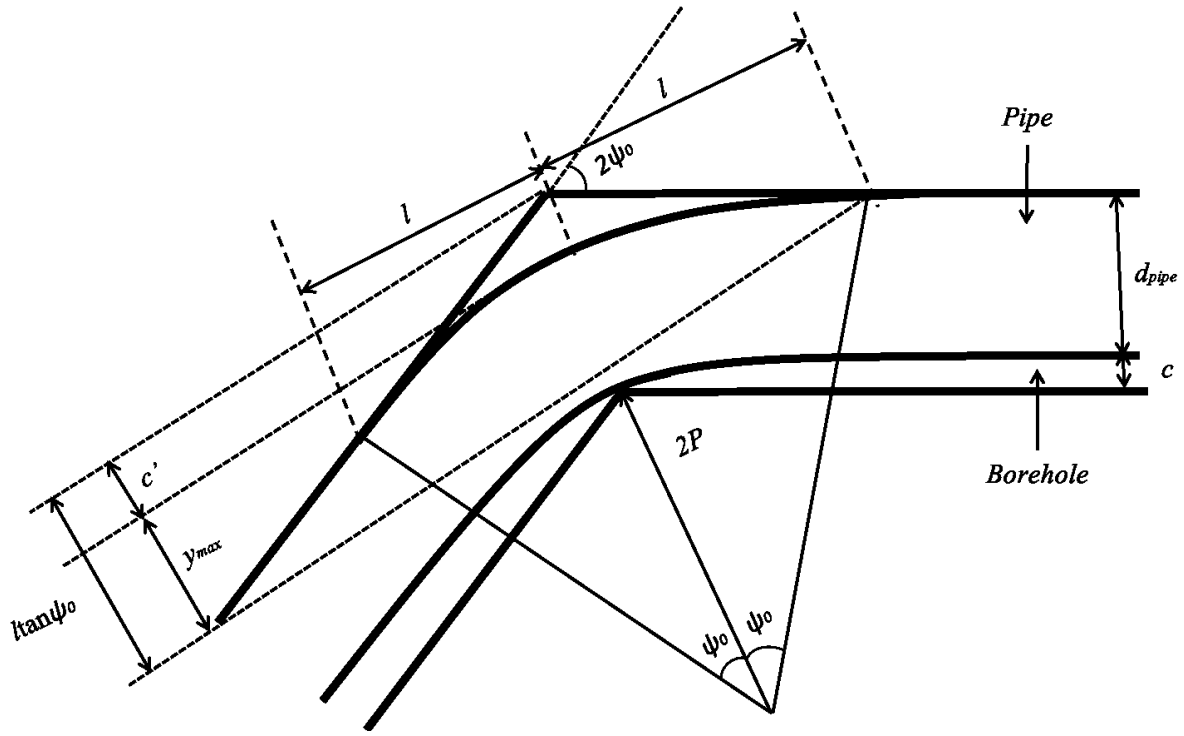

Figure 2-4. Model for calculating flexural forces acting on a pipe negotiating an angle in the borepath

Equations of flexible beams undergoing deflection are used to determine the contact load exerted on the center of the pipe (Frish-Fay 1962). y_{max}/l can be calculated using the following equations:

$$y_{\max} / l = (\sqrt{2} \sin\psi_0 \cos\phi_0 - \cos\psi_0 \Phi(p,\phi_0)) / (\sqrt{2} \cos\psi_0 \sin\phi_0 + \sin\psi_0 \Phi(p,\phi_0)) \quad [36]$$

$$\phi_0 = \cos^{-1} \sqrt{\sin\psi_0} \quad [37]$$

$$\Phi(p,\phi_0) = 0.8472 + F(p,\phi_0) - 2E(p,\phi_0) \quad [38]$$

The functions F (p, φ_0) and E (p, φ_0) are elliptic integrals and can be evaluated using mathematical handbooks (Abramowitz and Stegun 1965).

In order to calculate the force due to bending stiffness and change of direction, the contact load exerted on the pipe must be determined using the following equations:

$$P = (EI / l^2) \cos\psi_0 (\sqrt{2} \cos\psi_0 \cos\phi_0 + \sin\psi_0 \Phi(p,\phi_0))^2 \quad [39]$$

$$p = 1/\sqrt{2} \quad [40]$$

where P is the force from flexural stiffness (N); E is the Young's modulus (kPa) and I is the moment of inertia (m^4).

Finally, the force due to bending stiffness and change of direction at corner can be determined using the following equation:

$$\Delta T_{kif} = T_{k-1}((\cos\psi_k + \mu_b \sin\psi_k) / (\cos\psi_k - \mu_b \sin\psi_k) - 1) + 4P_k \mu_b (1 / (\cos\psi_k - \mu_b \sin\psi_k)) \quad [41]$$

where T_{k-1} is the pulling force in the force before entering the bend k in the borehole (N); P_k is the force from flexural stiffness (N) and ψ_k is the half the angle between the two line segments of the borehole at corner k (rad).

3. Study of Pressure Management in Horizontal Directional Drilling[1]

3.1. Introduction

During HDD, a significant amount of drilling fluid is used, which is one of the most critical components in the HDD process. Drilling fluid, often referred to as "mud," consists of water, bentonite, and occasionally additives to improve the drilling quality (Lu et al. 2012). The selection of the type of drilling fluid is dependent on a variety of factors, including safety concerns, environmental considerations, downhole pressure, and temperature (Bleier 1990). The tasks associated with drilling fluid include carrying cuttings out of the borehole and transporting them to the surface, cooling and lubricating the drill pipe and drill bit, stabilizing the borehole, controlling subsurface pressure, providing hydraulic power to the mud motor, and creating buoyant force for the drill pipe and product pipe (Ariaratnam et al. 2007; Shu et al. 2015; Shu and Ma 2015; Vajargah and van Oort 2015). However, there are some risks associated with the use of drilling fluids in HDD, including hydraulic fracturing and loss of circulation, which causes boreholes to collapse and mud loss, both of which are related to the pressure of drilling fluid (e.g., Wang and Sterling 2007; Murray et al. 2014). Therefore, it is of the utmost importance to ensure that there is a proper drilling fluid pressure management system in place during HDD construction.

Maximum allowable and minimum required drilling fluid pressures, and the annular pressure of drilling fluid, are essential during HDD (Bennett and Wallin 2008). As such, an accurate estimation of these pressures is crucial to the success of HDD projects. Generally, the annular pressure of drilling fluid should not exceed the maximum allowable drilling fluid pressure; otherwise, hydraulic fracturing may occur (Carlos et al. 2002). It is important to obtain an accurate prediction

[1] This chapter has been submitted to the Journal of Construction Engineering and Management and is under review.

of both pressures in order to mitigate the risks. Although there are several approaches to estimate the maximum allowable pressure for HDD, there is no consensus about which method is the most appropriate. In this chapter, the prediction of allowable pressure is broken down into analytical methods (closed-form equations), empirical method, experiments, and numerical simulation.

Minimum required pressure is another factor that must be considered in HDD construction and is defined as the pressure that is required for the drilling fluid to flow in the borehole (Lu et al. 2012). It is important to keep the minimum required pressure above the groundwater pressure, otherwise the borehole may collapse (Carlos et al. 2002). However, unlike maximum allowable pressure, the minimum required pressure is relatively small and sometimes ignored during projects.

In order to predict the annular pressure of the drilling fluid, the rheological properties of the drilling fluid should first be understood (Ariaratnam et al. 2004). The Bingham plastic, power law, and Herschel–Bulkley models are commonly used to predict drilling fluid behavior, and the estimations for annular pressure vary significantly depending on the rheological model (Okafor and Evers 1992). As a result, factors such as soil types and drilling fluid types play major roles in estimating the annular pressure during HDD operations.

Pressure management is one of the most important aspects of HDD projects. During construction, the maximum allowable and minimum required pressures and annular pressures are monitored to ensure that they stay in their acceptable pressure range (Carlos et al. 2002). Many factors, such as site condition, financial situation, and available technology, may affect the outcome of the project. The process of pressure management invovles performing a geotechnical investigation of the site and laboratory testing, estimating the maximum allowable and minimum required pressures, choosing the appropriate rheological model to estimate the annular pressure, monitoring and

comparing the maximum allowable and minimum required pressures to the annular pressure, and risk mitigation and contingency planning (Bennett and Wallin 2008).

During HDD construction, one of the major challenges is to prevent or minimize hydraulic fracturing from occurring. Hydraulic fracturing occurs when the annular pressure of drilling fluid exceeds the maximum allowable drilling fluid pressure. Therefore, to reduce the risks of hydraulic fracturing, the annular pressure should not exceed the maximum allowable drilling fluid pressure. However, there are currently several methods for calculating maximum allowable pressure and annular pressure. This chapter is focused on the review of methods available to estimate the maximum and minimum required drilling fluid pressures and possible models to estimate the annular pressure of drilling fluid, along with an overview of pressure management in HDD in order to provide a comprehensive understanding of hydraulic fracturing risk management in HDD construction. Closed form equations to estimate the pressures while drilling and their comparisons are discussed in detail, and some significant insights from the literature are provided for reference.

3.2. Different Approaches for Predicting Maximum Allowable Pressure

Maximum allowable drilling fluid pressure is defined as the maximum pressure soil can sustain without failure (Staheli et al. 2010). Shear failure and tensile failure are considered as the mechanisms that cause formation failure and its associated mud loss, and that create the potential for a blow-out (Yan et al. 2016). Two mechanisms are responsible for soil failure and drilling fluid loss: effective pressure acting on the borehole based upon the maximal allowable plastic zone around the borehole (Arends 2003), and hydraulic fracturing associated with tensile failure of surrounding soil (Kennedy et al. 2004a). The two primary factors that affect hydraulic fracturing in soil are borehole pressure and depth of cover (Lueke and Ariaratnam 2005). When the pressure in the borehole exceeds the strength of the surrounding strata, a frac-out condition occurs in which

drilling fluid escapes from the borehole and can migrate to the surface (Ariaratnam et al. 2003). Hydraulic fracturing is not only dependent on the drilling fluid pressure inside of the borehole, but also stress state and the strength parameters of the surrounding soil. Alfaro and Wong (2001) reported that the mechanisms of fracture in low-permeability soils appeared to be of a tensile failure mechanism. This was enhanced by the generation of pore pressure as the soil around the borehole was sheared due to the radial–tangential stress difference imposed by the injected pressure. Moore (2005) suggested that the maximum allowable mud pressure to prevent mud loss by hydrofracture is the pressure that initiates tensile stresses in the soil.

Two main approaches to estimate the maximum allowable pressure for drilling fluid are the empirical analysis and analytical solutions. The basis of the empirical approach is the statistical analysis of data from experiments and observations collected from both the laboratory and the field. During HDD, factors to consider include site-specific conditions and change in soil strata, which prevents the engineers from performing an accurate estimation of the maximum allowable pressure. Therefore, empirical equations may be used as an alternative approach for a quick and quantitative estimation. Analytical equations are more favorable as they denote exact solutions that can be used to study the behavior of the system with varying properties. In this context, four analytical models to predict maximum allowable drilling fluid pressure are discussed in detail. In addition, some of the examples of laboratory and field applications, as well as numerical approaches, are given to discuss further the available methods in use.

3.2.1. Analytical Approach

The analytical methods are the most accessible and popular approaches to estimate the maximum allowable pressure. These methods are often derived from mathematical models and theories, and presented as analytical solutions. In particular, four different analytical methods, the Delft equation

(Delft Geotechnics 1997), maximum strain solution (Verruijt 1993), the Queen's equation (Xia and Moore 2006), and the Yu and Houlsby (1991) equation are available in the literature. Overall, those four methods can be divided into different categories based on the criteria in the failure process that are stress development around a borehole (Delft equation and Yu and Holsby solution), strain development around a borehole (maximum strain solution), and coefficient of lateral earth pressure at rest (Queen's equation). A more detailed review can be found in the literature review section. The analytical methods are summarized in the table below.

Table 3-1. Summary of the equations used for the estimation of maximum allowable pressure

Method	Maximum Allowable Pressure	Application	Reference
Delft Solution	$p_{\max} = u + \left[\sigma'_0(1+\sin\varphi) + c\cos\varphi + c\cot\varphi\right]\cdot\left(\left(\frac{R_0}{R_{p,\max}}\right)^2 + \frac{\sigma'_0\sin\varphi + c\cos\varphi}{G}\right)^{\frac{-\sin\varphi}{1+\sin\varphi}} - c\cdot\cot\varphi$	Frictional Cohesive Soil (Sand and Gravel)	Luger and Hergarden (1988)
Maximum Strain Solution	$P_{\max} = \left\{\left[\varepsilon_{\theta,\max}\times\frac{2G}{P_0 + c\cdot\cot\varphi}\times\frac{1+m}{1-m}\right]^{\frac{1-m}{1+k}}\times\frac{2}{1+m}\left(P_0 + c\cdot\cot\varphi\right)\right\} - c\cdot\cot\varphi$	Frictional Cohesive Soil (Sand and Gravel)	Keulen (2001)
Queen's Equation	$P_i = c_u + 0.5(3K_0 - 1)P_0 - c_u\ln\left(\left(\frac{R_0}{R_{p,\max}}\right)^2 + \left(\frac{c_u + 1.5(K_0-1)P_0}{G}\right)\right)$ $P_i = c_u + 0.5(3 - K_0)P_0 - c_u\ln\left(\left(\frac{R_0}{R_{p,\max}}\right)^2 + \left(\frac{c_u + 1.5(1-K_0)P_0}{G}\right)\right)$	Purely Cohesive Soil (Clay)	Xia and Moore (2006)
Yu and Houlsby Solution	$R_{\lim} = \frac{(m+a)[Y + (a-1)P_{\lim}]}{a(1+m)[Y + (a-1)P_0]}$	Frictional Cohesive Soil (Sand and Gravel)	Yu and Houlsby (1991)

Overall, the Delft method, the maximum strain method, and the Yu and Houlsby solution are more applicable to frictional cohesive soil, such as sand and gravel, whereas the Queen's equation is more applicable to purely cohesive soil such as clay, but there is no consensus on which method yields the most accurate results. Currently, the Delft solution is favored in the HDD industry; however, it was reported that the use of the Delft solution underestimates the maximum allowable pressures (e.g. Duyvestyn 2004; Moore 2005; Wang and Sterling 2006; Elwood et al. 2007; Ngan 2015), and requires judgment and accurate geotechnical data (Conroy et al. 2002). When assumptions regarding geotechnical conditions and drilling practices are invalid, results are likewise unsatisfactory. The Delft solution provides a mechanism for predicting maximum allowable pressures. Minimum required pressures for drilling and reaming must also be calculated and compared against maximum allowable pressure to assess hydro-fracture risks (Bennet 2009).

Moreover, a case study published by Yan et al. (2016) focused on the prediction and comparison of the maximum allowable pressure of horizontal boreholes drilled for the Qin River crossing with HDD having a driven length of 1,750 m. Based on the geological data, the Delft equation and the Queen's equation (based on tensile failure) were employed to calculate the maximum allowable annular pressure of the pilot hole. These predictions were compared with the actual pressure data collected in the field, and Yan et al. (2015) observed that the Queen's equation was conservative, and the limits of the Delft equation could not express the strength limitation of overburden soil. They used a finite element model where plane strain conditions were assumed, and the Mohr–Coulomb failure criterion was used to define the development of the plastic zone in soil. Based on the analyses, Yan et al. (2016) concluded increasing the ground surface load would raise the borehole allowable pressure at which point fracturing would occur.

3.2.2. Empirical Approach

The empirical approach to predict the maximum allowable pressure considers fewer variables because they are statistical interpretations of the observations; therefore, the results obtained by these methods should be considered carefully before using, as they may not represent site specific conditions. In general, the easiest way to predict the maximum allowable pressure using the empirical approach is to use 1 psi (7 kPa) per foot (0.305 m) of burial depth as the estimated maximum allowable pressure (Xia 2009). However, the calculations should not be regarded as an accurate representation of the maximum allowable pressure, but rather a reference for quick analysis since they do not consider soil properties.

3.2.3. Experiments

A very limited number of laboratory tests to investigate the maximum allowable pressure for drilling fluid in HDD are reported. Existing laboratory experiments mainly focus on characterization of the hydraulic fracturing of soils. Murdoch (1993a, b, c) used laboratory tests to characterize the fracture face and fracture propagation from a vertical borehole. He suggested a new parameter, fracture toughness, be implemented in the equations to calculate pressure acting in the fracture that is very difficult to measure in practice. Elwood (2008) conducted a series of experiments on a poorly graded sand that was compacted in a cell having dimensions of 0.8 m × 0.32 m × 0.78 m for small-scale tests and 2.0 m × 2.0 m × 1.5 m for large-scale tests to investigate the maximum allowable pressure of a drilling fluid by hydraulic fracturing and consequent mud loss. The test procedure included drilling a horizontal borehole with a specially designed tube while applying constant overburden pressure on the top boundary. The length of the boreholes differed depending on the boundary conditions. A bentonite-water mixture was used as drilling fluid and was pumped into the borehole until hydraulic fracturing was observed at the surface or mud loss was observed by the change in recorded drilling fluid pressure. The main purpose of the

large-scale tests was to investigate the effectiveness of various maximum allowable pressure estimation methods such as the Delft solution.

Similar to the experiments of Elwood (2008), a set of large-scale tests were performed by Xia (2009). The main objective was to simulate different overburden pressures and to gain a better understanding of the impact of a layered granular system. It was also expected that the large-scale tests produced a better simulation of the conditions encountered in actual field applications. One of the advantages of large-scale tests is minimizing boundary effects. The major conclusion drawn from these experiments and analyses is that there was no consensus on a better prediction of the maximum allowable drilling pressure, since Elwood reported a better comparison of the laboratory data with the Delft solution than Yu and Houlsby, while Xia (2009) indicated the opposite. It must be considered that there is only limited laboratory data available, and these approaches need to be supported with additional experimental data.

3.2.4. Numerical Analysis

Although non-complex and easy methods to determine the maximum allowable pressure are preferred in practice, due to the uncertainties of the ground, there are some attempts to better characterize the soil behavior. Kennedy et al. (2004a) performed a two-dimensional finite element analysis using elastic plate theory to investigate the maximum allowable drilling pressure when drilling in clays by neglecting both the gradient in the earth and mud pressure across the cavity and the potential for shear failure around the cavity. They modeled the elastic response of undrained clays and introduced a new equation to calculate the maximum drilling pressure, which is defined as the pressure that initiates the hydraulic fracture. Kennedy et al. (2004b) used a finite element model to investigate hydraulic fracture, considering elasto-plastic conditions critical for its presence when drilling through clay soil. They also focused on the reliability of elastic plate

theory and plasticity theory with a Mohr-Coulomb failure criterion to predict the drilling slurry pressures that lead to tensile failure of the surrounding soil. It was concluded that when the soil response was elastic, the elastic plate theory was efficient to predict the springline stresses and decreases in tangential crown stresses, while plasticity theory accurately calculated the tangential stresses once the soil at the crown or springline had yielded (Kennedy et al. 2004b). The increase in stress after the yield indicated that hydraulic fracture, associated with tensile rupture of the soil, is no longer an issue once plastic yielding has occurred at the crown or springline of the borehole.

Kennedy et al. (2006) extended their work to investigate behavior of the filter-cake, which is developed under internal borehole drilling fluid pressure of HDD using the finite element method used in Kennedy et al. (2004b). More specifically, the analysis focused on the drilling fluid pressures that initiate tensile stresses in the filter cake. The filter cake is mostly formed around the borehole by sand layers and drilling fluid. The effects of filter cake thickness, borehole depth, and the location of the maximum tensile stresses were investigated and discrepancies noted due to the relatively late response of tangential tension in the filter cake to mud loss.

Elwood (2008) used the numerical model that was developed by Kennedy et al. (2004, a, b; 2006) with improvements in the material properties based on physical data. The major conclusions of the study were that it is unclear if the filter cake plays a major role in the borehole's ability to withstand a blowout, and the growth of the filter-cake does not have any impact on the borehole's ability to withstand a blowout.

3.3. Annular Pressure of drilling fluid

To reduce the risk of hydraulic fracturing in HDD, the annular pressure of drilling fluid should be less than the maximum allowable pressure of drilling fluid at all times. Therefore, an accurate calculation of annular pressure of drilling fluid is another essential part of HDD construction. The

majority of the new drilling methods, such as managed pressure drilling (MPD), also rely on precise prediction of the annular pressure profiles. For instance, the frictional pressures encountered by the drilling fluid in the annulus need to be carefully understood and characterized in order to properly manage back-pressure during surface-pressure managed MPD techniques. The annular pressure of drilling fluid has two main components: hydrostatic and friction loss. Hydrostatic pressure is caused by the weight of the drilling fluid, while friction loss pressure is caused by the internal friction within the fluid and the friction with the wall of the borehole (Osbak 2011). The hydrostatic component of the annular pressure of drilling fluid, $P_{s,}$ is calculated as follows:

$$P_s = \rho g h \qquad [42]$$

where ρ is the density of the drilling fluid (kg/m^3), g is the acceleration due to gravity (m/s^2), and h is the vertical distance from the point of interest in the hole to the top of the fluid within the hole (m).

Friction loss pressure in the pipe is highly related to the viscosity of drilling fluid, which is defined as the fluid's resistance to flow, and whether the flow regime is laminar or turbulent (Osbak 2011). In the case of drilling fluid, the flow regime is almost always laminar. Moreover, if a fluid has a constant viscosity under constant temperature and pressure, it is defined as a Newtonian fluid, which has a linear relationship between shear stress and shear rate, and the line passes through the origin. Drilling fluids, however, are not Newtonian because they are composed of both liquid and solid particles. Therefore, the relationship between shear stress and shear rate is not linear for drilling fluid since the viscosity changes when the shear rate changes (Viloria Ochoa 2006).

Properties such as yield point, plastic viscosity, and apparent viscosity are crucial in evaluating drilling fluid efficiency for cleaning boreholes while drilling (Kelessidis et al. 2006). Rheological models are intended to provide assistance in characterizing these properties. No single, commonly used model completely describes rheological characteristics of drilling fluids over their entire shear rate range. Knowledge of rheological models, combined with practical experience, is necessary to understand fully fluid performance (API 2010). A plot of shear stress versus shear rate is used to graphically depict a rheological model, as shown in Figure 2. There are three rheological models to predict the characteristics of a non-Newtonian fluid, which are the Bingham plastic (1922); power law, also known as Ostwald-de Waele relationship (Blair et al. 1939); and Herschel–Bulkley (1926). After the rheological model for drilling fluid is determined, the friction loss pressure can be calculated. However, it is not an easy task to determine which model is the best for a particular HDD construction since there are factors, such as type of drilling fluid and drilling fluid properties that need to be considered. To better understand the effect of the properties of drilling fluid, annular pressures for different models are calculated and compared against field data.

3.3.1. Rheological Models for Drilling Fluid

The Bingham plastic model is the simplest model of the three rheological models for drilling fluids. The model assumes true plastic behavior for the drilling fluid, and is represented by a straight line on the shear stress-shear rate relationship, as shown in Figure 3-1.

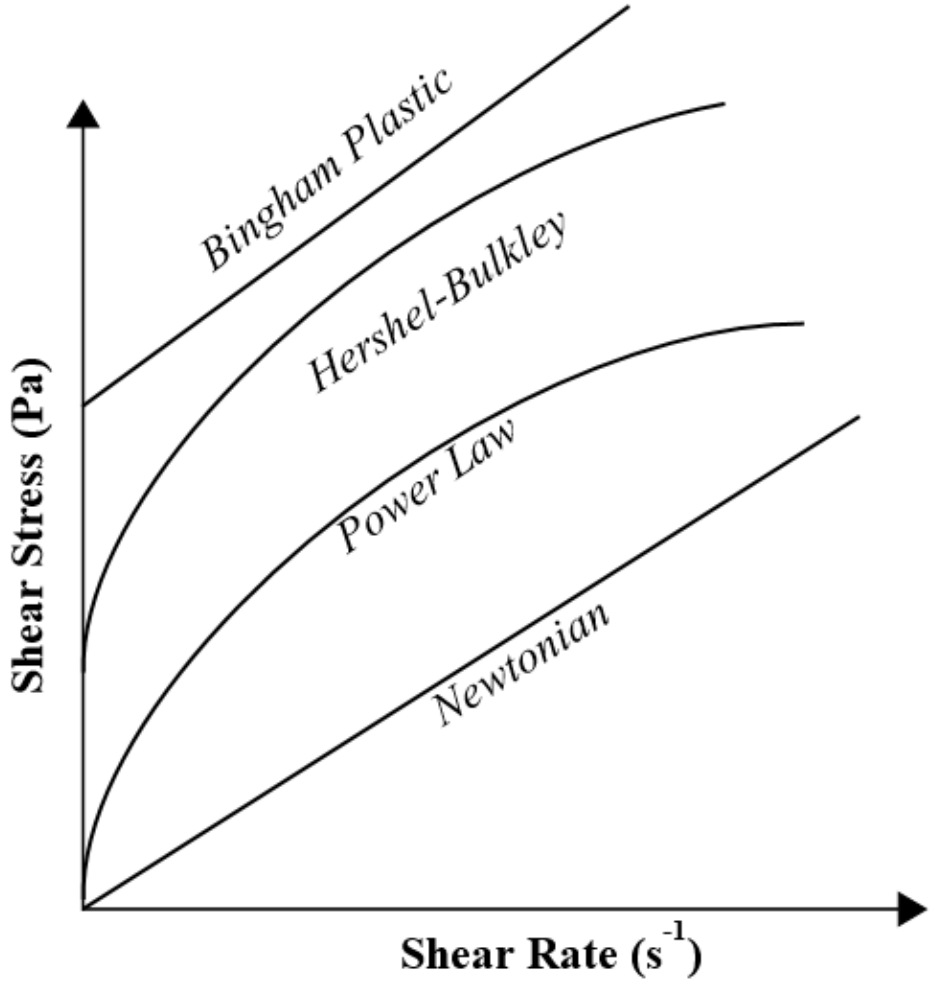

Figure 3-1. Rheological models for drilling fluids

For Bingham plastic fluids, the yield point is a critical point, and the fluid can flow only if the shear stress exceeds the yield point. Therefore, the model is not accurate at predicting fluid behavior at low shear rate. As such, this model is best suited for water-based cement slurries. The power law model on the other hand, follows a non-linear relationship between shear stress and shear rate with the curved line passing through the origin. It is more accurate at describing drilling fluid with low shear rate when compared to the Bingham plastic model. Therefore, the model is better suited for drilling fluids with zero yield stress, such as polymer-based drilling fluid (Zamora et al. 1993). The biggest drawback of this model is that it does not account for the yield stress in

the drilling fluid, and does not have a term for yield point. The Herschel-Bulkley model (1926) is more complex when compared to the Bingham plastic and power law models because it considers both the plastic behavior and yield stress of drilling fluids. It has three components: yield stress, flow index, and consistency index, and it was proposed as an improvement to the other two models. The summary of models is given in Table 3-2.

Table 3-2. Summary of pressure drop in annulus for different rheological properties of drilling fluid

Model	Shear stress	Pressure drop in annulus
Bingham Plastic (e.g. Ariatranam et al 2007)	$\tau = YP + PV \cdot \gamma$ τ: shear stress (Pa), γ: shear rate (1/s), YP: yield point (Pa), PV: plastic viscosity	$P_a = \left(\frac{14580 \times PV \times V_a}{\left(ID_{HOLE} - OD_{DP} \right)^2} + \frac{1.83 \times YP}{\left(ID_{HOLE} - OD_{DP} \right)} \right) \times L$ V_a: average mud velocity in the annulus (m/s), ID_{HOLE}: diameter of hole or inside diameter of casing (mm), OD_{DP}: outside diameter of the drill pipe or drill collar (mm), L is the length (m)
Power Law (API 2017)	$\tau = k\gamma^n$ n: flow index (dim.), k: consistency index	$P_a = \sum \left(\frac{1.076 \rho_a V_a^2 fL}{10^5 d_{hyd}} \right)_j$ ρ_a: fluid density in the annulus (lbm/gal), V_a: fluid velocity (ft/min), f: fanning friction factor (dim.), d_{hyd}: hydraulic diameter (in.)
Herschel-Bulkley (1926)	$\tau = \tau_y + k\gamma^n$	Calculated using computer software

While all models described are suitable methods for estimating the annular pressure, Bingham plastic and the power law models are more common in practice, although the Herschel-Bulkley model has been tested and is well received because of its high accuracy. However, the Herschel-Bulkley model is not widely used because of its complexity compared to the Bingham plastic and the power law models (Subramanian and Azar 2000). Numerous experimental works in directional drilling revealed that the Herschel-Bulkley model gives the best fit to the data, and can accurately predict the friction loss through both the eccentric and the concentric pipes (Simon 2004; Ofei 2016; Okafor and Evers 1992).

Using a polymer/calcium carbonate system and mixed metal hydroxide system as drilling fluids, Simon (2004) concluded that the Bingham plastic model overestimates pressure drop, the power law model underestimates pressure drop, and the Herschel-Bulkley Model is the most accurate at describing fluid behavior. The findings of Langlinais et al. (1983) are similar to those of Simon (2004).

Baumert et al. (2005) reported that the current HDD practice of calculating annular frictional pressure loss caused by drilling fluid drag based on the assumption of concentric annular flow of a Bingham plastic fluid is overly conservative. Consequently, critical design parameters, such as depth of cover, which affects crossing length, and drilling equipment size, which is selected based on anticipated pulling load, cannot be optimized (e.g., Chehab and Moore 2012).

3.3.2. Annular Pressure Loss for Different Rheological Models

To quantify the differences in the rheological models and associated pressure drop, a viscosity test was performed in the laboratory using a mud consisting of 3% bentonite in a Fann 35A viscometer at 3, 6, 100, 200, 300 and 600 RPM. The experiment follows the procedure as recommended in API 13D-1 (2010) to measure shear stress-shear rate relationship. The three models were used to

calculate the shear stresses and were compared with the measured values as shown in Figure 3-2 (a). Three data sets were recorded and the average was taken. According to the results, the Herschel-Bulkley model gave the best fit to the measured data for the shear stress. Pressure losses with increasing borehole length were calculated based on different rheological models using a mud consisting of 3% bentonite and an outer borehole diameter of 228.6 mm and an inner diameter of 127.0 mm as reported in Ariaratnam et al. (2003). The results are given in Figure 3-2 (b). It was seen that the pressure drops from the Baroid method were higher than both the power law and Herschel-Bulkley models, and the Ariatranam method has the lowest pressure drop of them all. Nevertheless, based on the shear stress-shear rate relationship, the Bingham model should have a higher pressure drop since it has a higher shear stress than the other two models.

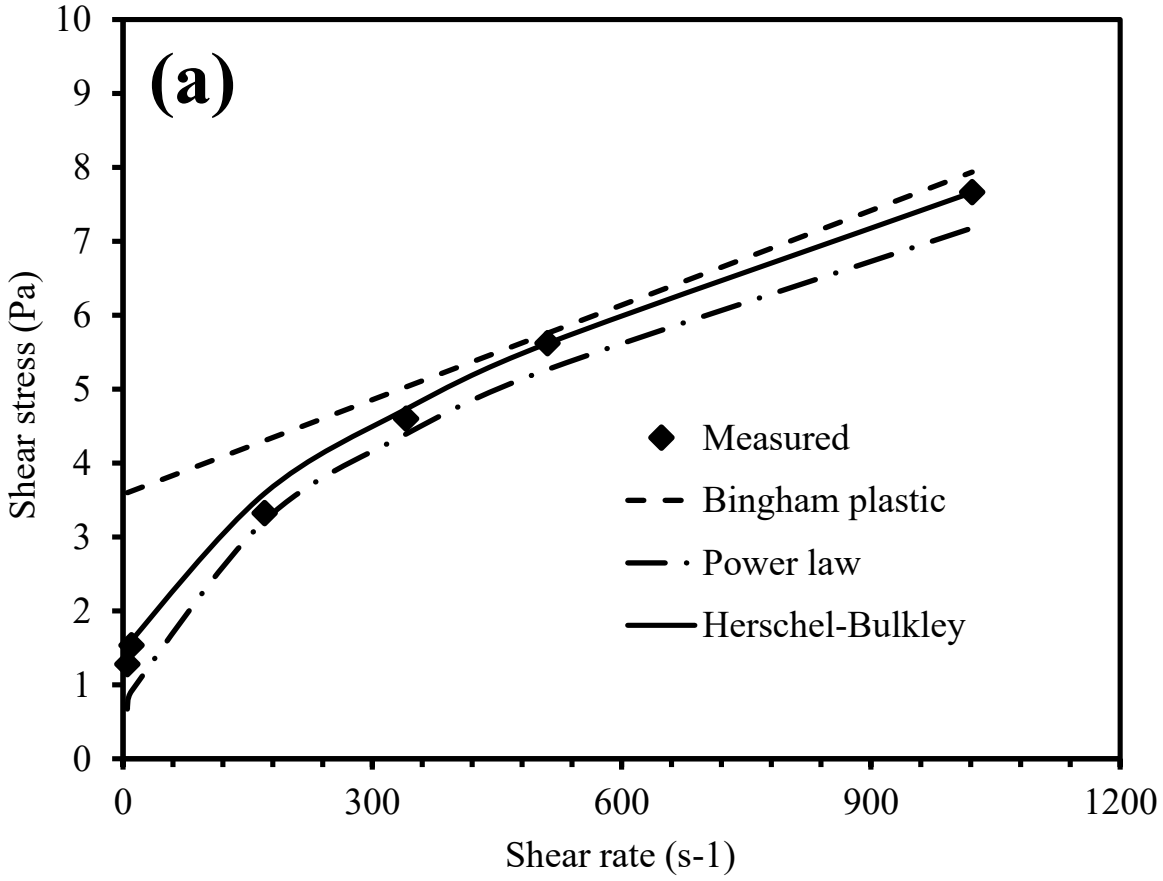

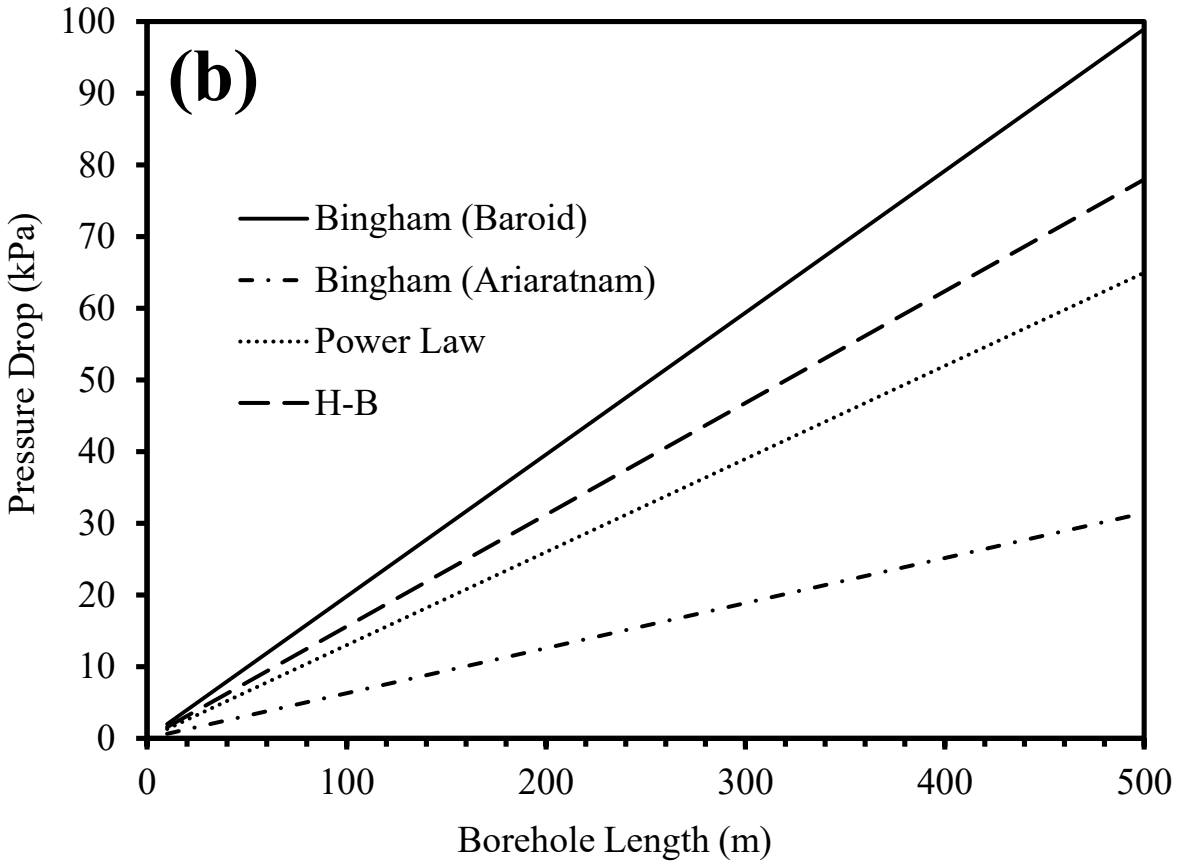

Figure 3-2. Comparison of rheological models: (a) Shear stresses; (b) Pressure loss

To better understand the differences between the models to predict annular pressure during operation of HDD, field data is used for comparison. Rostami (2017) used field data collected from a case in northwestern Alberta, Canada to compare annular pressure predicted by Bingham Plastic model and Power Law model to the measured annular pressure. The rheological parameters used for Bingham Plastic model and Power Law model are derived from different shear rate ranges (3, 6, 100, 200, 300 and 600 RPM). The field data can be found in Rostami's paper (2017). Based on the comparison, it is concluded that Bingham Plastic model is more accurate at predicting annular pressure at low shear rate range of 100 – 200 RPM and overestimates the annular pressure by 30% on average at high shear rate range of 200 – 300 and 300 – 600 RPM; Power Law model can

properly predict annular pressure at shear rate range of 3 – 600 RPM and the most accurate prediction results from a shear rate range of 6 – 100 RPM.

Despite the differences in the rheological models, there are also additional factors that may affect the annular pressure loss, such as the geometry of the borehole and spatial and temporal changes in the geometry (Marken et al. 1992). If all variables could be held constant, the annular pressure loss in any eccentric annulus is less than those of calculated for the concentric annulus. When considering all possible annular geometries during a drilling operation, the probability of a completely concentric annulus is very small at any given time. This alone makes the elementary calculations, which assume a concentric annulus, only an estimation at best. Unlike laboratory studies, the eccentricity of a well annulus does not remain constant with time. Under the appropriate conditions, the change from a concentric to eccentric annulus can facilitate the transition to turbulent flow.

3.4. Pressure Management and Monitoring

The first step in pressure management for HDD involves performing geotechnical site investigations to obtain various soil parameters and useful site information, such as formation of the site, obstacle layout, soil type, deformation properties, and groundwater table behavior (Hair III 1995). Laboratory experiments are usually conducted to determine the physical and engineering properties of soils, such as unit weight, moisture content, particle size distribution, and undrained shear strength. These factors are needed to maintain the stability of the borehole during drilling. In addition, site investigations are necessary to determine the likelihood of potential risks of construction (Allouche et al. 2001).

After all necessary parameters are acquired from the geotechnical investigation and laboratory tests, the maximum allowable pressures can be estimated using one of the approaches mentioned

above, and the minimum required pressure can be predicted using the minimum required pressure equation. The third step in pressure management is to obtain annular pressure from drilling fluid behavior. The complete procedure for pressure management is shown in Figure 3-3.

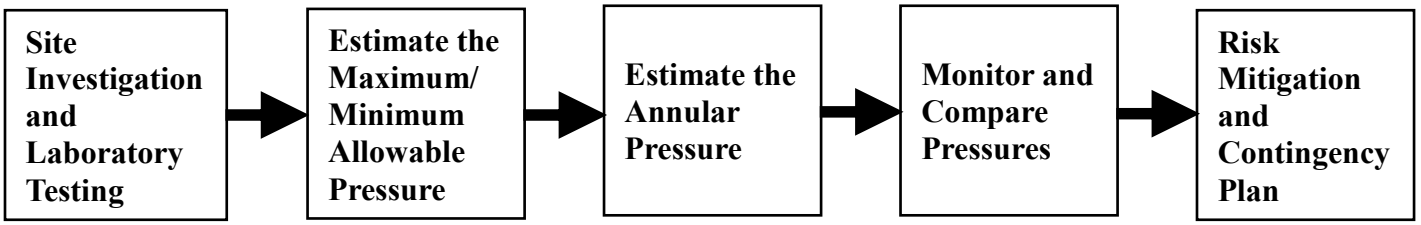

Figure 3-3. The general procedures in pressure management

One of the most important steps of pressure management in HDD is real time monitoring (Verwey 2013). Typically, the annular pressure is monitored by a pressure sensor that is attached several meters behind the bit (Royal et al. 2010) and can be shown on a live display that is attached to the driller's equipment. The pressure sensor is an integral part of the downhole steering system that can provide real time monitoring of annular pressure and give early warnings of hydraulic fracturing. In addition, the annular pressure is often shown together with the maximum allowable and minimum required pressures for the operator to compare and analyze. Therefore, the operator can make quick adjustments to the drilling operation in order to ensure the annular pressure stays in range. If the annular pressure is not within the acceptable range of the maximum allowable and minimum required pressures, the operation should be stopped and investigated for potential risks and failures.

There are some associated risks and failures, such as hydraulic fracturing, surface heave (Lueke and Ariaratnam 2005), loss of circulation of the drilling fluid, and soil collapse involved in HDD operations, and failure can lead to potential project delay, safety issues, and financial penalties. Therefore, an effective contingency and risk mitigation plan is needed to ensure the success of the operation. Tanzi and Andreasen (2011) examined the various contingency planning elements that

were considered during the project's planning, design, and construction phases of an HDD project in Raritan River, and concluded that the two most important stages for minimizing and mitigating risks are the pre-construction and mid-construction phases. For the pre-construction phase, a proper borehole geometry design, a careful and thorough geotechnical investigation, and good drilling fluid and tool selection are needed to help reduce potential risks. For the mid-construction phase, an effective hydraulic fracturing detection system, a good communication system, and an appropriate pressure monitoring system are useful in minimizing potential risks. In addition, other risk mitigation techniques, such as relief wells and piezometers, are beneficial in reducing risks.

Conversely, contingency planning is critical in dealing with HDD related disasters after they have occurred. For any HDD construction, there should be several general contingency plans in place to cope with different types of failures, such as pilot hole failure, drilling fluid failure, pullback failure, and reaming failure. Each contingency plan should include general corrective action, response personnel and equipment, clean up procedure, authority notification procedure, and follow up investigation (Tanzi and Andreasen 2011).

3.5. Conclusion

This chapter focuses on the pressure management of drilling fluid in HDD and its components. Observations from the literature conclude that it is difficult to predict accurately the maximum allowable and minimum required pressures and annular pressure during HDD operations because of the uncertainties of the ground. Among the four most commonly used models to estimate the maximum allowable drilling fluid pressure, the most favorable approach is the Delft solution, although there is a tendency to overestimate the maximum allowable pressure. An extensive data set from both actual HDD projects and laboratory experiments is recommended to investigate further the reliability of these models.

Currently, the three most adopted rheological models to characterize the behavior of the drilling fluid are the Bingham plastic, power law, and Herschel–Bulkley, and the last has been proven to give better fit to the experimental data. However, the industry prefers the Bingham plastic model and the power law model due to their convenience and accessibility, and they are still accurate at predicting certain drilling fluid behavior. The selection of the rheological model has a significant effect on the calculation of the pressure loss along a borehole.

There are many components involved in pressure management, from field investigation to pressure estimation and pressure monitoring, and it is crucial to prioritize and have a proper management plan for each step. To minimize the risk associated with the drilling, a proper monitoring system is needed. Ultimately, an effective communication scheme, an ongoing collaboration, and good engineering judgement are what makes a successful HDD operation.

4. Study of Overcut Ratio in Horizontal Directional Drilling

4.1. Introduction

There are three main steps in the construction process of HDD: 1) drilling of the pilot hole, 2) reaming of the pilot hole, and 3) pulling back of pipe string (Colwell and Ariaratnam 2003). During reaming of the pilot hole, the borehole has to be made large enough so the pipe can be pulled back through the borehole and the ratio of borehole diameter to pipe diameter is called the overcut ratio. As previous research indicated, a decrease in overcut ratio will result in an increase in total pullback force (Polak et al., 2004). Therefore, the total pullback force is minimized by increasing the overcut ratio. However, the pilot hole has to be reamed multiple times, which in turn makes the project more costly and time consuming. As a result, an optimal overcut ratio for HDD installation is very important for developing a better design guideline.

As a rule of thumb, the borehole is to be reamed 1.5 times larger than the pipe diameter (Popelar et al. 1997) and this is widely accepted as the industry standard. The recommended back ream borehole diameters are given in Table 4-1 (Ariaratnam and Allouche 2000). However, relatively little research has been done in the area of improvement to overcut ratio in HDD and there is no formal study that proves whether the industry standard overcut ratio of 1.5 is suitable or not. Thus, the goal of this paper is to analyze the role of overcut ratio in HDD and to provide a theoretical basis of the optimal overcut ratio.

Table 4-1. Recommended Backream Hole Diameter (Popelar et al. 1997)

Nominal pipe diameter (mm)	Backream hole diameter (mm)
50	75-100
75	100-150
100	150-200
150	250-300
200	300-350
250	350-400
≥300	At least 1.5 times product outer diameter

The overcut ratio in HDD is directly related to the total pullback force, as an increase in overcut ratio will result in a decrease in total pullback force. A total of four methods are used to estimate total pullback force in HDD: the PRCI (Pipeline Research Council International) method, the ASTM F1962 method, the NEN 3650 method, and the Pipeforce method developed by Polak and Cheng (2007). All four methods are compared and discussed in this paper but the Pipeforce method is further analyzed to determine the effect of the overcut ratio in HDD installation. The Pipeforce method is straightforward but incorporates all the major factors that affect the total pullback force; and three important components are considered in the calculation: force due to borehole friction, force due to fluidic drag and force due to change in direction and bending stiffness. Furthermore, steel pipes and PE pipes are analyzed separately as they behave differently underground during HDD installation.

4.2. Predicting Total Pullback Force

The overcut ratio is defined as the ratio of the diameter of the borehole to the external diameter of the pipe (Royal et al. 2010) and is a crucial factor affecting total pullback force. To properly evaluate the effect of overcut ratio in HDD, one has to review the role of overcut ratio in total pullback force.

4.2.1. Methods for Estimating Total Pullback Force

Currently, there are six major analytical models used by the industry to estimate total pullback force: Driscopipe method, Drillpath method, PRCI method, ASTM F1962 method, NEN 3650 method and Pipeforce method (Cai et al. 2017). Each of the models has its unique properties and advantages and disadvantages. However, based on the study done by Cai et al. (2017), it was concluded that both Driscopipe method and Drillpath method underestimate the total pullback force for both steel and polyethylene (PE) pipes. Therefore, this chapter will only discuss four models that are used to calculate total pullback force in HDD: PRCI method, ASTM F1962 method, NEN 3650 method and Pipeforce method. A detailed review of each method can be found in the literature review section and the four methods are summarized in the table below.

Table 4-2. Summary of the equations used for the estimation of total pullback force

Method	Maximum Allowable Pressure	Application	Reference
PRCI Method	$T_2 = T_1 + \mid frict^1 \mid + DRAG \pm wL\sin\theta$ (straight section) $T_2 = T_1 + 2\times \mid frict^2 \mid + DRAG \pm wL_{arc}\sin\theta$ (curved section)	Steel	Huey et al. (1996)
ASTM F1962 Method	$T_A = \exp(v_a\alpha)(v_a w_a(L_1 + L_2 + L_3 + L_4))$ $T_B = \exp(v_b\alpha)(T_A + v_b \mid w_b \mid L_2 + w_b H - v_a w_a L_2 \exp(v_a\alpha))$ $T_C = T_B + v_b \mid w_b \mid L_3 - \exp(v_b\alpha)(v_a w_a L_3 \exp(v_a\alpha))$ $T_D = \exp(v_b\beta)(T_C + v_b \mid w_b \mid L_4 - w_b H - \exp(v_b\alpha)(v_a w_a L_4 \exp(v_a\alpha)))$	PE	ASTM F1962 (2011)
NEN 3650 Method	$T_{total} = T_1 + T_2 + T_{3a} + T_{3b} + T_{3c}$ $T_1 = f_{install} \times L_{roller} \times Q \times f_1$ $T_2 = f_{install} \times L_2 \times (\pi D_0 \times f_2 + Q_{eff} \times f_3)$ $T_{3a} = f_{install} \times L_{arc} \times (\pi D_0 \times f_2 + Q_{eff} \times f_3)$ $T_{3b} = f_{install} \times 2 \times q_r \times D_0 \times \frac{\pi}{\lambda} \times f_3$ $T_{3c} = f_{install} \times L_{arc} \times g_t \times f_3$	Steel	Netherlands Standardization Organization (2007)
Pipeforce Method	$T_i = T_{ig} + T_{is} + T_{id} + \sum_{k=1}^{i-1} \Delta T_{kif}$ $T_{ig} = (w_p \mu_g \cos\alpha_0 + w_p \sin\alpha_0)(L - \sum_{k=0}^{i-1} L_k)$ $T_{is} = \sum_{k=0}^{i-1}(\mid L_k w \mu_b \cos\alpha_k \mid + L_k w \sin\alpha_k)\,;\ T_{id} = \sum_{k=0}^{i-1} f_a L_k$ $\Delta T_{kif} = T_{k-1}(\frac{\cos\psi_k + \mu_b \sin\psi_k}{\cos\psi_k - \mu_b \sin\psi_k} - 1) + 4P_k \mu_b (\frac{1}{\cos\psi_k - \mu_b \sin\psi_k})$	Steel and PE	Cheng and Polak (2007)

4.2.2. Comparison of Different Methods

Generally, there are five force components involved in calculating total pullback force: 1) force due to friction between pipe and borehole/ground surface; 2) force due to fluidic drag; 3) force due to Capstan Effect; 4) force due to bending stiffness and 5) force due to change in direction. Nonetheless, not all methods consider all the force components in the calculation. For example, PRCI method does not consider the force due to friction between pipe and ground surface, force due to Capstan Effect and force due to change in direction; ASTM F1962 method does not include force due to bending stiffness and force due to change in direction; and NEN 3650 method does not consider force due to change in direction. However, Pipeforce method considers all the five components mentioned above. The results are summarized in Table 4-3 below.

Table 4-3. Force components considered by different models

	Force due to friction	Force due to fluidic drag	Force due to Capstan Effect	Force due to bending stiffness	Force due to change in direction
PRCI	✗	✓	✗	✓	✗
ASTM	✓	✓	✓	✗	✗
NEN 3650	✓	✓	✓	✓	✗
Pipeforce	✓	✓	✓	✓	✓

Moreover, the four methods mentioned above perform differently with different pipe materials, namely steel and PE. Based on a study conducted by Cai et al. (2017), it is determined that both PRCI method and NEN 3650 method are suitable for steel pipe but overestimate pulling force in PE pipe; ASTM F1962 method is suitable for PE pipe but underestimates pulling force in steel pipe and Pipeforce method is suitable for both steel and PE pipes.

This chapter is focused on using the Pipeforce method to provide a better understanding of the role of the overcut ratio in HDD and to find a theoretical value of overcut ratio that is the most appropriate for HDD installation. The overcut ratio is evaluated by the value of total pullback force and the correlation between overcut ratio and total pullback force is explored. Since steel and PE pipes have different mechanical properties, they are discussed separately. In addition, the effect of overcut ratio on fluidic drag force, force due to bending stiffness and change of direction and most importantly, total pullback force are analyzed and discussed. Closed form equations to estimate total pullback force and their comparisons are discussed in detail.

4.2.3. Case Study

Two cases are studied to evaluate the models for predicting total pullback force in HDD. The case studies are divided into two categories: steel and PE. For steel pipe, PRCI, NEN 3650 and Pipeforce models are compared. The field data is taken from Yangtze River crossing project (2009) in China where two steel pipes were installed separately using an American Augers and the initial field data is presented in Table 4-4. For PE pipe, ASTM, NEN 3650 and Pipeforce models are compared. The field data is taken from HDD installations at University of Waterloo (2001) in Canada where three PE pipes were installed using Ditch Witch 2040 drill rig and the initial field data is presented in Table 4-4. The soil type for both case studies is fine sand. In addition, some assumptions are made for entry and exit angles, standard dimension ratio and diameter to radius ratio with regards to the field data.

Table 4-4. Input parameters for pipe crossing calculations

	Steel	PE
Entry angle (degrees)	7	8
Exit angle (degrees)	10	11
SDR (Standard Dimension Ratio)	17	17
Pipe density (N/m^3)	78000	9200
Slurry density (N/m^3)	12000	14800
Water density (N/m^3)	9800	9800
Friction coefficient between pipe and borehole	0.24	0.24
Friction coefficient between pipe and ground	0.6	0.6
Fluidic drag coefficient (Pa)	345	345
Young's modulus of pipe, E (GPa)	200	0.7
Diameter to radius ratio	1200	40
Average pipe velocity, vp (m/s)	0.026	0.05
Average fluid velocity, v (m/s)	0.0098	0.0606
Total discharge of the drilling fluid, Q (m^3/s)	0.0063	0.0020
Viscosity ($N\ s/m^2$)	0.02	0.02

Using overcut ratio of 1.5 and field data in Table 4-4 (Cai et al. 2017), a comparison of total pullback force between different methods for steel and PE pipes at different pipe diameters are shown in Figure 4-1 (a) and 4-1 (b). According to the results, for steel pipes, the total pullback forces for PRCI and NEN 3650 method are identical up to around 700 mm pipe diameter; however, Pipeforce method shows a slightly larger total pullback force at large pipe diameter. This phenomenon may be caused by the force due to change of direction increasing at larger pipe diameter. For PE pipes, ASTM F1962 and Pipeforce methods are shown to produce similar results while NEN 3650 method is shown to have overestimate the total pullback force. Overall, the findings from Figure 4-1 (a) and 4-1 (b) agree with the study conducted by Cai et al. (2017). Therefore, it can be established that Pipeforce method is a valid model for calculating total pullback force in HDD.

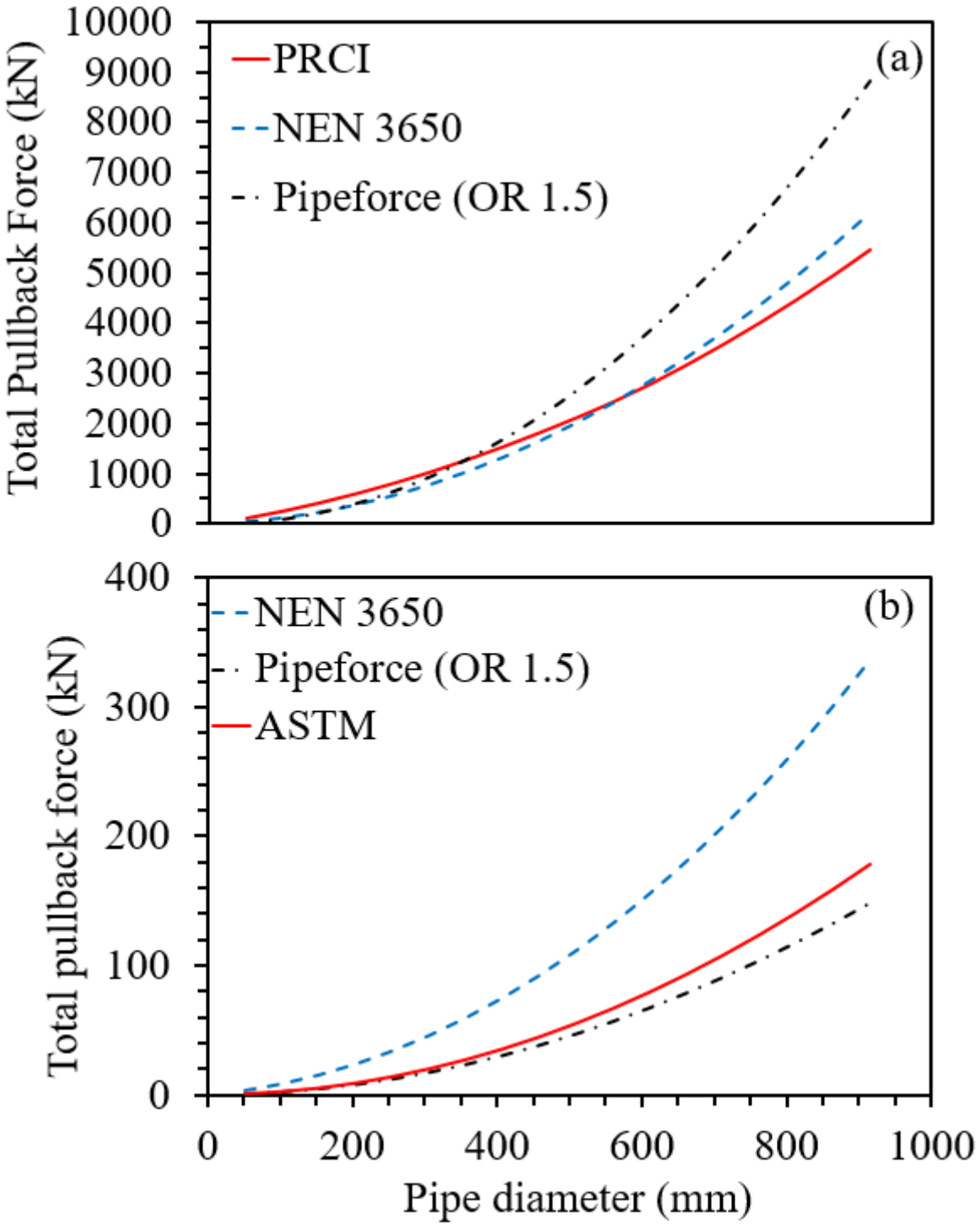

Figure 4-1. Comparison of total pullback force for different methods: (a) Steel; (b) PE

4.3. The Application of Overcut Ratio in Pipeforce Method

In order to determine the overcut ratio in HDD, the borehole diameter and pipe diameter have to be decided before construction. However, out of all the four methods discussed in this paper, only Pipeforce method involves both borehole diameter and pipe diameter (the other three models only incorporate pipe diameter in their calculations). As a result, Pipeforce method is the only available method to analyze the role of overcut ratio in HDD.

In Pipeforce method, the total pullback force is calculated as a sum of four different forces: friction force between pipe and soil, friction force between pipe and borehole, fluidic drag force and force due to bending stiffness and change of direction. However, based on Eq. [28] and [29], the overcut ratio has a negligible effect on both friction force between pipe and soil and friction force between pipe and borehole as those forces are greatly influenced by the weight of pipe and friction coefficient. On the other hand, the overcut ratio significantly affects the fluidic drag force, and force due to bending stiffness and change of direction as both borehole diameter and pipe diameter appear in the calculations.

In order to analyze the effect of overcut ratio on HDD, a study of two pipeline installation projects involving different pipe materials (steel and PE) is conducted. Two generic borehole profiles were constructed: Figure 4-2 (a) shows the borehole profile for steel pipe crossing and Figure 4-2 (b) shows the borehole profile for PE pipe crossing. The initial parameters used in calculation are taken from Yangtze River Crossing project in 2009 and HDD installation at University of Waterloo in 2001 (Cai et al. 2017). They are presented in Table 4-4. Additionally, there are a few assumptions made for the calculation: 1) all pipes of different sizes have the same SDR; 2) the bend radius of pipe remains constant during installation (as a common rule of thumb, for steel pipe, the bend radius is 1200 times of pipe diameter; for PE pipe, the bend radius is 40 times of pipe

diameter); 3) the force due to ground friction is neglected; and 4) the pipe is either filled with 100% water or no water during installation.

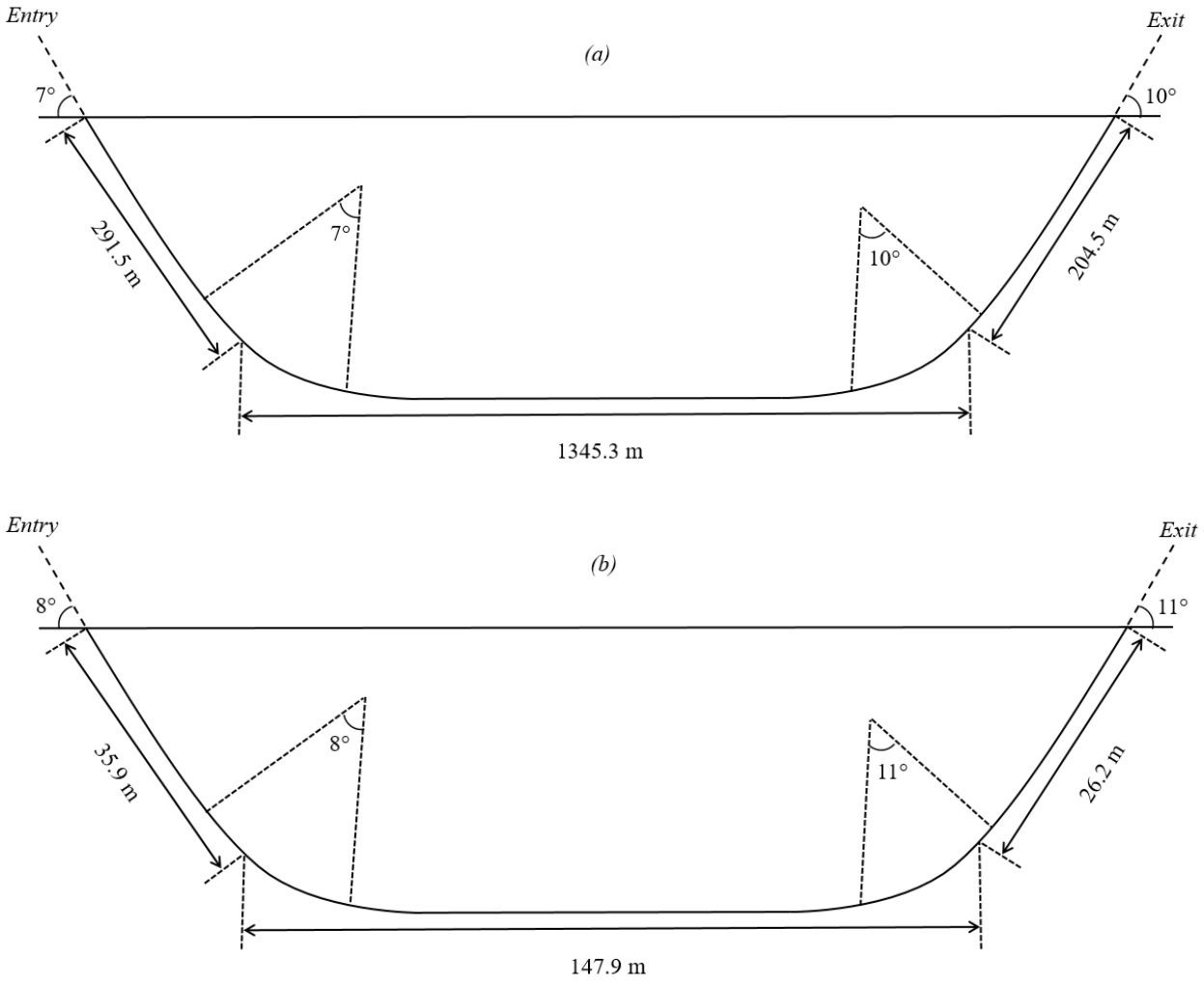

Figure 4-2. Designed borehole profile for pipe crossing: (a) Steel pipe; (b) PE pipe

4.3.1. Steel Pipe

The field data from Yangtze River Crossing project used in the calculations is presented in Table 4-4. Figure 4-3 (a) shows the change in fluidic drag forces at various overcut ratios for steel pipe. The fluidic drag force ranges from 0.1 kN to 0.5 kN for overcut ratio between 1.2 to 2.0 and is not affected by the size of the pipe. It displays a non-linear trend and the fluidic drag force decreases as the overcut ratio increases.

Figure 4-3 (b) demonstrates the effect of overcut ratio on force due to change in direction at pipe diameters between 0.1016 m to 0.9144 m for steel pipe. The force due to change in direction ranges from 15 kN to 24000 kN at different pipe diameters for overcut ratio between 1.2 to 2.0. The graph shows a non-linear relationship between force due to change in direction and overcut ratio at different pipe diameters: as overcut ratio increases, the force due to change in direction decreases. However, the rate of change in force due to change in direction varies drastically for different pipe diameters. For example, at 0.1016 m of pipe diameter, the force due to change in direction ranges from around 15 kN to 300 kN and the average rate of change is 32 kN per 0.1 overcut ratio; at 0.9144 m of pipe diameter, the force due to change in direction ranges from 1200 kN to 24000 kN and the average rate of change is 2533 kN per 0.1 overcut ratio. Nonetheless, the rate of change in force due to change in direction is non-linear and it becomes less and less significant as the overcut ratio increases.

Figure 4-3 (c) shows the relationship between total pullback force and overcut ratio at pipe diameters between 0.1016 m to 0.9144 m for steel pipe. The total pullback force ranges from 70 kN to 29000 kN at different pipe diameters for overcut ratio between 1.2 to 2.0. The graph displays a non-linear relationship between total pull force and overcut ratio and the overall trend is similar to Figure 4-3 (b): as overcut ratio increases, the total pullback force decreases; and the rate of change in total pullback force is different for different pipe diameters. At 0.1016 m of pipe diameter, the total pullback force ranges from 70 kN to 350 kN and the average rate of change is 31 kN per 0.1 overcut ratio; at 0.9144 m of pipe diameter, the total pullback force ranges from 5900 kN to 29000 kN and the average rate of change is 2567 kN per 0.1 overcut ratio. The rate of change in total pullback force shows a non-linear trend and becomes less significant as the overcut ratio increase.

4.3.2. PE Pipe

The field data from HDD installation at University of Waterloo used for calculation of PE pipes is presented in Table 4-4. Figure 4-4 (a) shows the change in fluidic drag forces at various overcut ratios for PE pipes. The force due to fluidic drag ranges from 0.05 kN to 0.25 kN for overcut ratio between 1.2 to 2.0. Similar to steel pipe, the size of the pipe does not affect the fluidic drag force with change in overcut ratio. The relationship between fluidic drag force and overcut ratio is non-linear.

Figure 4-4 (b) shows the effect of overcut ratio on force due to change in direction at pipe diameters between 0.1016 m to 0.9144 m for PE pipes. Compared to steel pipes, the force due to change in direction is much smaller and it ranges from 0.1 kN to 88 kN at different pipe diameters for overcut ratio between 1.2 to 2.0. Similar to steel pipe, a non-linear relationship between force due to change in direction and overcut ratio is presented: the force due to change in direction decreases with an increase in overcut ratio. However, the rate of change in force due to change in direction is significantly different for different pipe diameters. For example, at 0.1016 m of pipe diameter, the force due to change in direction ranges from around 0.1 kN to 1 kN and the average rate of change is 0.1 kN per 0.1 overcut ratio; at 0.9144 m of pipe diameter, the force due to change in direction ranges from 10 kN to 88 kN and the average rate of change is 8.7 kN per 0.1 overcut ratio. Similar to steel pipe, the rate of change in force due to change in direction shows a non-linear trend and it becomes smaller and smaller as the overcut ratio increases.

Figure 4-4 (c) shows the relationship between total pullback force and overcut ratio at pipe diameters between 0.1016 m to 0.9144 m for PE pipes. The total pullback force ranges from 2 kN to 217 kN at different pipe diameters for overcut ratio between 1.2 to 2.0. The figure shows same trend as steel pipe: as overcut ratio increases, the total pullback force decreases; and the rate of

change in total pullback force is different for different pipe diameters. At 0.1016 m of pipe diameter, the total pullback force ranges from 2 kN to 3 kN and the average rate of change is 0.1 kN per 0.1 overcut ratio; at 0.9144 m of pipe diameter, the total pullback force ranges from 138 kN to 216 kN and the average rate of change is 8.7 kN per 0.1 overcut ratio. The rate of change in total pullback force is non-linear and becomes smaller and smaller as the overcut ratio increase.

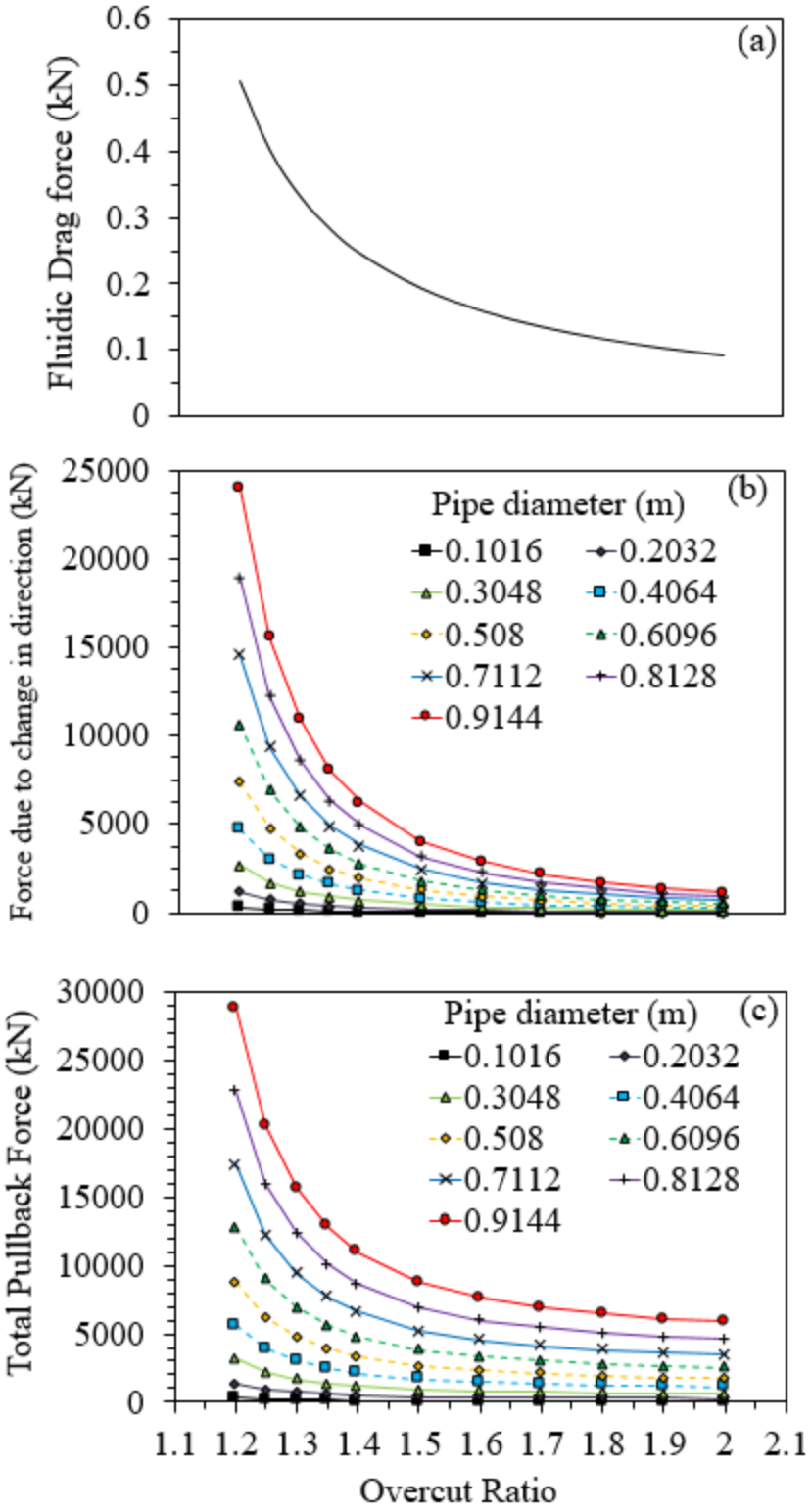

Figure 4-3. Different forces in Pipeforce Method for steel pipe: (a) Fluidic drag force, (b) Force due to change in direction and (c) Total pullback force

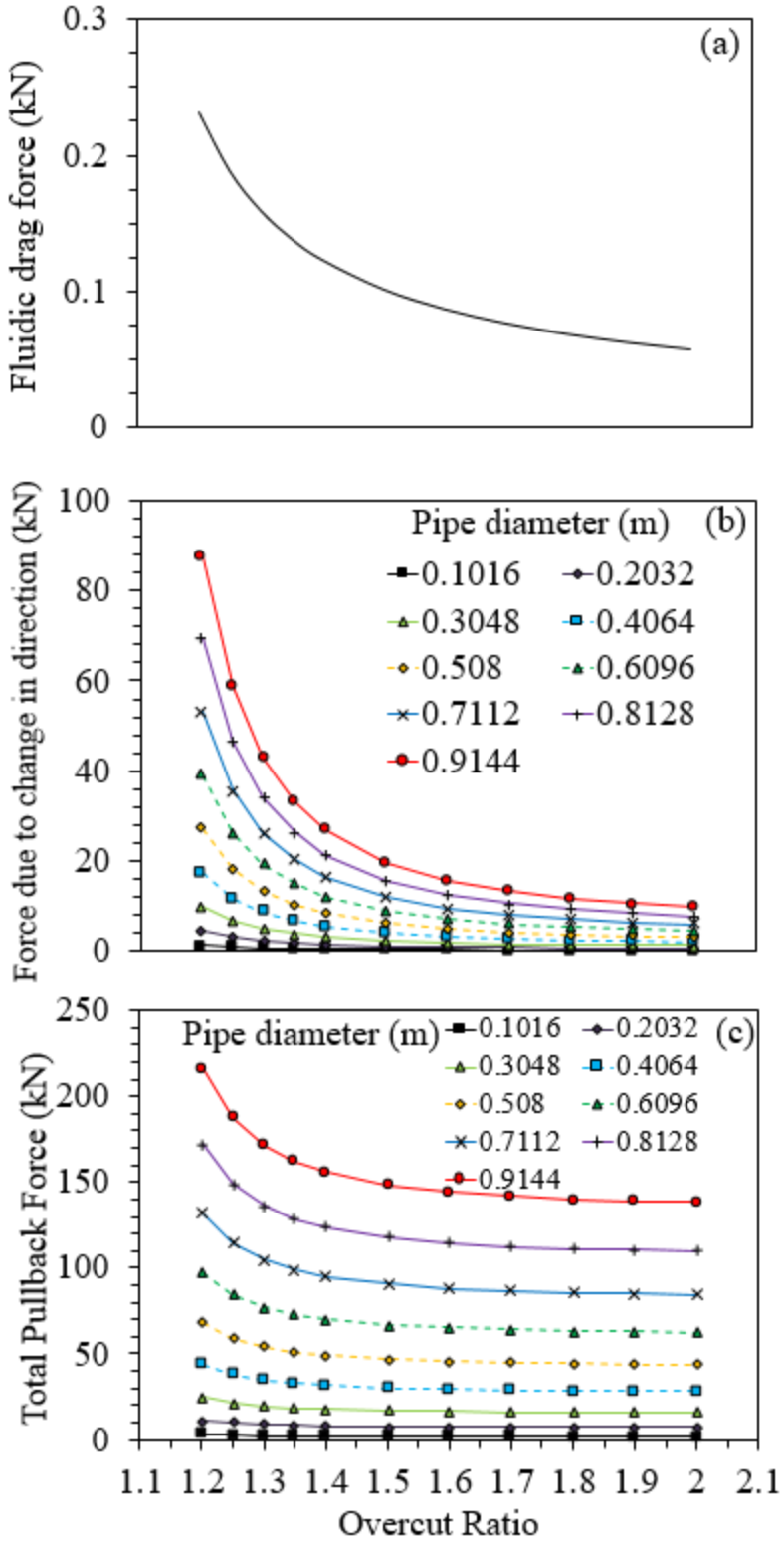

Figure 4-4. Different forces in Pipeforce Method for PE pipe: (a) Fluidic drag force, (b) Force due to change in direction and (c) Total pullback force

4.3.3. Comparison of Steel and PE

For steel pipe, the effect of fluidic drag force is vastly insignificant and on average comprises about 0.1% of the total pullback force. However, the force due to change in direction makes up around 20 - 85% of total pullback force depending on the overcut ratio: as the overcut ratio increases, the percentage of force due to change in direction with respect to total pullback force decreases. The rest of forces are made up by force due to borehole friction, which makes up around 15 – 80% of total pullback force. At 1.5 overcut ratio, the force due to change in direction is about 48% and the force due to borehole friction is about 52% with respect to total pullback force. Therefore, in steel pipe, the total pullback force is mostly dependent on the force due to change in direction if the overcut ratio is smaller than 1.5 and it is mostly dependent on the force due to borehole friction if the overcut ratio is larger than 1.5.

For PE pipe, the effect of fluidic drag force is not negligible at lower pipe diameters (0.254 m and below) and it makes up approximately 1 – 7% of total pullback force at different overcut ratios. Nevertheless, as pipe diameter increases, the effect of fluidic drag force becomes less and less meaningful and on average consists of about 0.2% of the total pullback force at higher pipe diameters (0.3048 m and above). The force due to change in direction makes up about 7 – 40% of total pullback force depending on the overcut ratio: with lower overcut ratio having a higher percentage of total pullback force. However, the majority of forces is comprised of force due to borehole friction which makes up around 55 – 92% of total pullback force. As a result, the force due to borehole friction is the more influential force in PE pipes HDD installation.

4.4. Discussion

Currently, the most widely accepted methods for calculating total pullback force are PRCI method and ASTM F1962 method for steel and PE pipes respectively (Yan et al. 2018). Figures 4-5 (a)

and 4-5 (b) show the comparison of PRCI and Pipeforce methods for steel pipes and the comparison of ASTM and Pipeforce methods for PE pipes respectively. For steel pipes, the PRCI method does not follow the trend of Pipeforce method at one particular overcut ratio. For example, at lower pipe diameters, the PRCI method is similar to the Pipeforce method at overcut ratio of 1.5; at higher pipe diameters, the PRCI method is similar to the Pipeforce method at overcut ratio of 1.8 and beyond. However, for PE pipes, the ASTM method displays a similar trend to the Pipeforce method at an overcut ratio of 1.3.

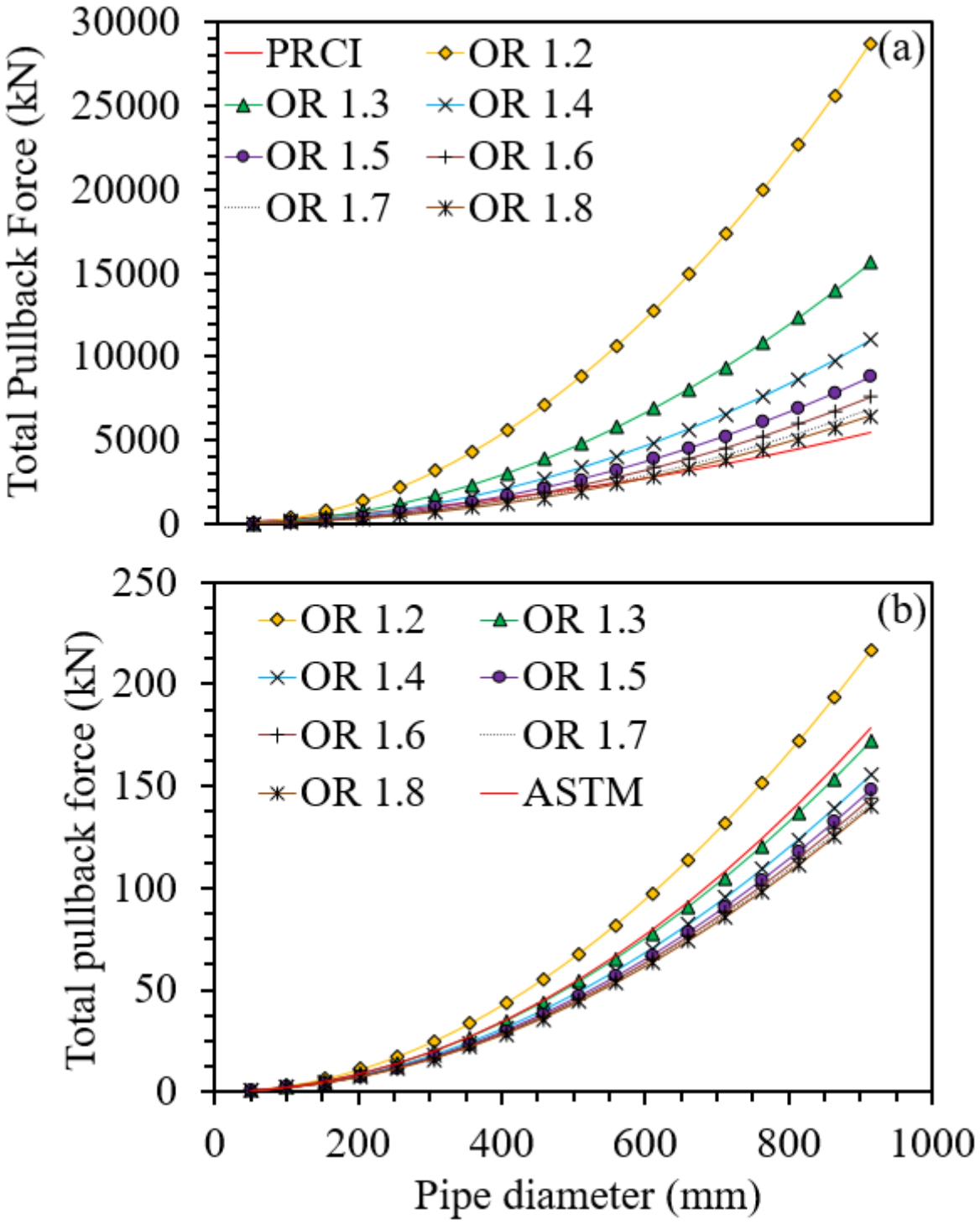

Figure 4-5. Comparison of total pullback force for PRCI, ASTM and Pipeforce Methods at different overcut ratio: (a) Steel; (b) PE

As mentioned before, the HDD industry currently use an overcut ratio of 1.5 as a rule of thumb (Popelar et al. 1997) for HDD construction, especially during larger diameter pipe installation (larger than 250 mm OD). Using Pipeforce Method, both Figures 4-3 (c) and 4-4 (c) display the relationship between total pullback force and overcut ratio for steel and PE pipes: as overcut ratio increases, the total pullback force decreases. However, it can be observed from Figures 4-3 (c) and 4-4 (c) that the change in total pullback force is the most significant from 1.2 to 1.5 overcut ratio for steel pipes and 1.2 to 1.3 overcut ratio for PE pipes. As the overcut ratio reaches beyond 1.5 and 1.3 for steel and PE pipes respectively, the change in total pullback force becomes more and more minimal for steel and PE pipes respectively. Table 4-5 shows the percent change in total pullback force with respect to different overcut ratios. The percent change in total pullback force is the percent decrease in total pullback force when the overcut ratio increases and it is calculated by averaging the percent change in total pullback force from pipe diameters 0.0508 mm to 0.9144 mm.

Table 4-5. Percent change in total pullback force at different overcut ratios

Overcut Ratios	Percent Change (Steel)	Percent Change (PE)
1.1 to 1.2	70.7%	51.5%
1.2 to 1.3	46.0%	20.7%
1.3 to 1.4	30.1%	9.4%
1.4 to 1.5	20.1%	4.9%
1.5 to 1.6	13.7%	2.9%
1.6 to 1.7	9.6%	1.8%
1.7 to 1.8	6.9%	1.2%
1.8 to 1.9	5.1%	0.9%
1.9 to 2.0	3.8%	0.6%

For steel pipe, the percent change in total pullback force is 13.7 % for overcut ratio from 1.5 to 1.6; and for PE pipe, the percent change in total pullback force is 9.4% for overcut ratio from 1.3 to 1.4. Both of these percent changes in total pullback force are less than 15%. Therefore, for sand, the author concluded that the impact of overcut ratio on total pullback force is more substantial if the overcut ratio is smaller than 1.5 for steel pipe and 1.3 for PE pipes. On the other hand, the engineers can use the percent change in total pullback force to justify the increase or decrease in overcut ratio.

Using overcut ratio of 1.5 as a reference point, normalization curves of total pullback force with respect to overcut ratio at various pipe diameters for steel and PE pipes can be obtained. They are shown in Figures 4-6 (a) and (b) for installation with water and Figures 4-7 (a) and (b) for installation without water. The percentage on the Y-axis is calculated by dividing the difference between total pullback force at one particular overcut ratio and total pullback force at 1.5 overcut ratio to total pullback force at 1.5 overcut ratio. Pipe diameter of 0.1016 m is neglected in the calculation. All four figures demonstrate that the normalization curves converge on the same curve at different pipe diameters; therefore, different pipe diameters do not affect the percent change in total pullback force for the different overcut ratio. Overall, for both steel and PE pipes installation with or without water, the change in percentage of total pullback force is more drastic at overcut ratio smaller than 1.5. For example, for steel pipe installation with water, the total pullback force at 1.4 overcut ratio is 25% more than the total pullback force at 1.5 overcut ratio and the total pullback force at 1.6 overcut ratio is only 13% less than the total pullback force at 1.5 overcut ratio; for PE pipe installation with water, the total pullback force at 1.4 overcut ratio is 5% more than the total pullback force at 1.5 overcut ratio and the total pullback force at 1.6 overcut ratio is only 2.7% less than the total pullback force at 1.5 overcut ratio. Additionally, the normalization

curves presented in Figures 4-6 (a) and (b) and Figures 4-7 (a) and (b) can be used as a reference for a fast and simple estimation of total pullback force during HDD planning and construction.

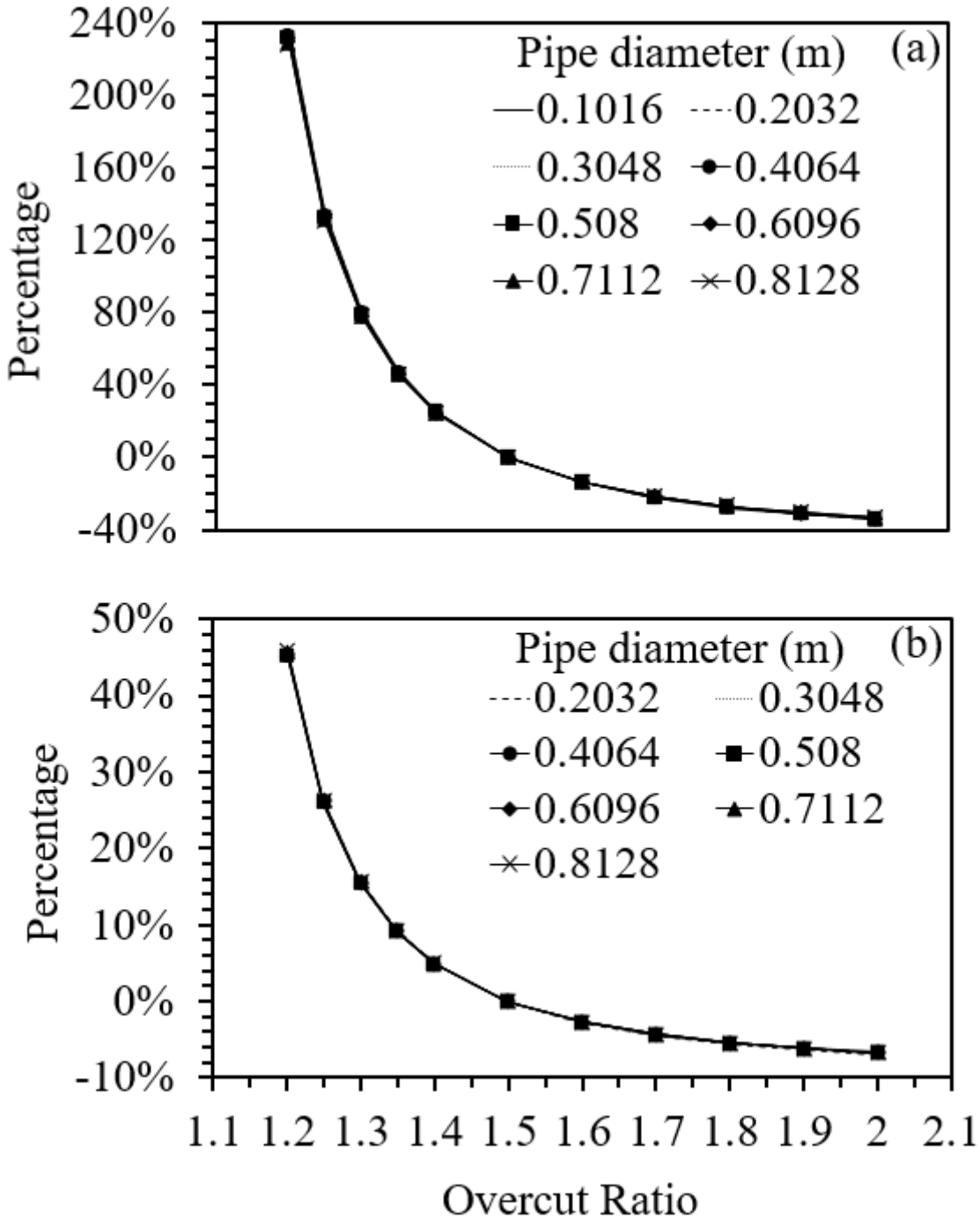

Figure 4-6. Percent change in total pullback force with respect to total pullback force at 1.5 overcut ratio (assuming pipe is filled with water during installation): (a) Steel; (b) PE

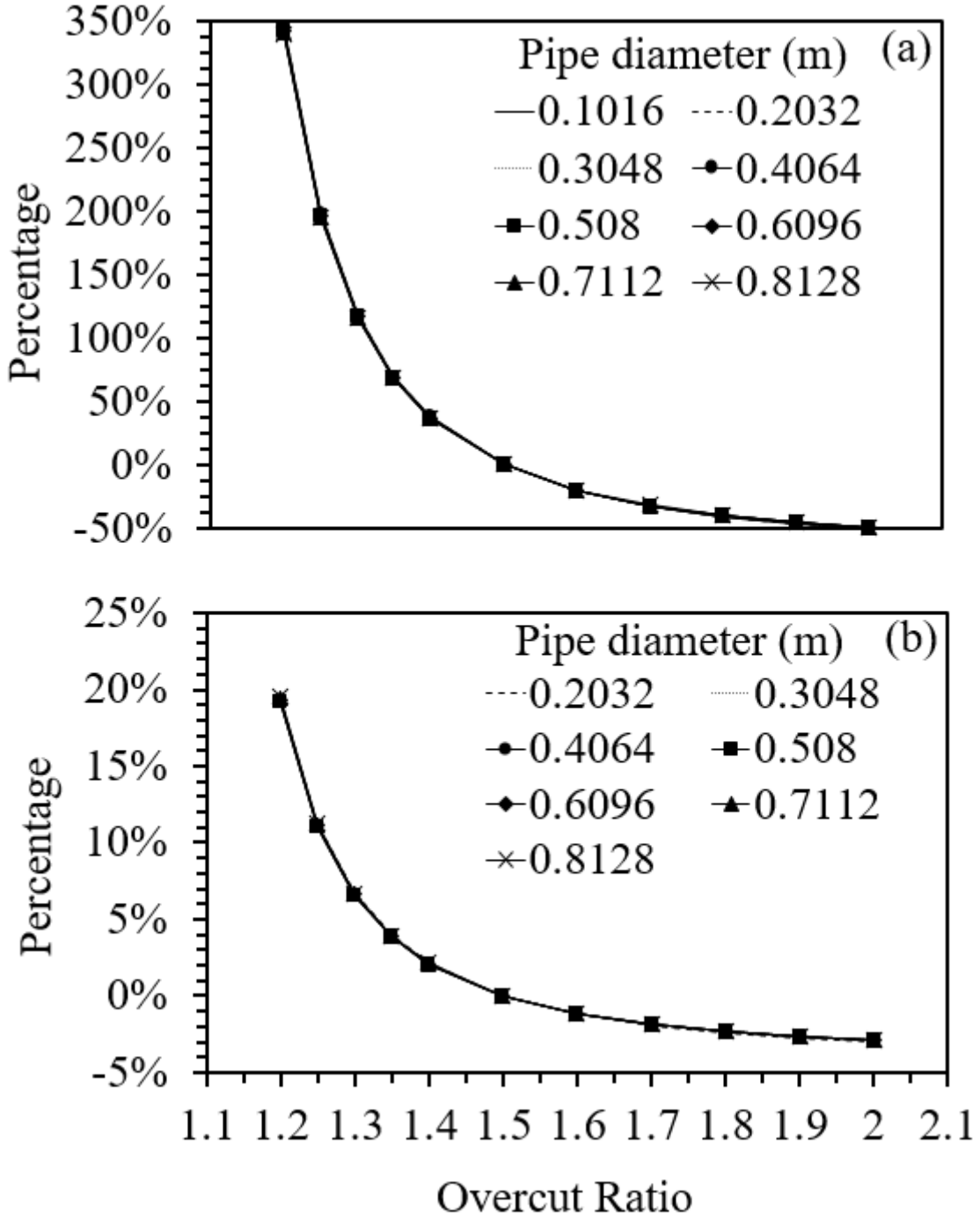

Figure 4-7. Percent change in total pullback force with respect to total pullback force at 1.5 overcut ratio (assuming there is no water inside pipe during installation): (a) Steel; (b) PE

4.5. Conclusion

This chapter summarizes the findings on the role of overcut ratio in HDD using Pipeforce method. From the literature review, it is concluded that both PRCI method and NEN 3650 method are suitable for steel pipe; ASTM F1962 method is suitable for PE pipe and Pipeforce method is suitable for both steel and PE pipes. Three different force components, force due to borehole friction, force due to fluidic drag and force due to change in direction and bending stiffness, are analyzed and discussed for steel and PE pipes; and the results show the total pullback force is dependent on the force due to change in direction if the overcut ratio is smaller than 1.5 and dependent on the force due to borehole friction if the overcut ratio is larger than 1.5 for steel pipe; and the total pullback force is dependent on the force due to borehole friction for PE pipes no matter the overcut ratio.

Another analysis of normalized data of total pullback force and overcut ratio demonstrates that pipe diameter has a negligible effect on the percent change in total pullback force for different overcut ratios; and the produced normalization curve can be used to quickly evaluate the total pullback force during HDD construction planning.

However, the analysis and calculation do not represent the whole picture of the role of the overcut ratio in HDD installation as more factors, such as soil condition, need to be considered. Nonetheless, the result is a good indicator on what can be expected when determining the overcut ratio, which will ultimately lead to the improvement of design guideline for HDD. Overall, based on the analysis and calculation of the Pipeforce method, theoretical values of overcut ratio in HDD installation can be established for both steel and PE pipes. As a result, for sand, the author recommends an overcut ratio of 1.5 for steel pipes in HDD installation; however, for PE pipes, an overcut ratio of 1.3 is adequate.

5. Summary, Conclusions and Future Research

5.1. Summary

Horizontal Directional Drilling (HDD) is becoming more and more popular for underground construction. Compared to the traditional open-cut method, it is cheaper, more efficient and causes less surface disruption. However, there are still risks associated with HDD such as hydraulic fracturing and drilling fluid loss; and there is still room for improvement with the design guideline. This study presented different methods for estimating various pressures during HDD construction and described the role of overcut ratio in HDD.

To minimize the risk of hydraulic fracturing and drilling fluid loss in HDD, there has to be a superb pressure management system in place. There are three pressures that are essential during HDD construction: they are the maximum allowable pressure, minimum required pressure and annular pressure of drilling fluid. Four different methods, the Delft equation (Delft Geotechnics 1997), maximum strain solution (Verruijt 1993), the Queen's equation (Xia and Moore 2006), and the Yu and Houlsby equation (1991) are compared and analyzed for maximum allowable pressure; and three different rheological models, Bingham Plastic model (1922), Power Law model (1939), and Herschel–Bulkley model (1926) are discussed and compared for annular pressure loss in HDD. Finally, a general procedure for pressure management in HDD is proposed.

Overcut ratio is the ratio of borehole diameter to pipe diameter and it is an important criteria to consider during the pullback phase of HDD construction. Four different methods for estimating total pullback force, PRCI method, ASTM F1962 method, NEN 3650 method and Pipeforce method are presented; and a case study is conducted for comparison. Moreover, Pipeforce method is used to examine the role of overcut ratio in both steel and PE pipes; and two case studies are

carried out for steel and PE pipes respectively. In the end, the author gives his recommendation for the appropriate overcut ratio for steel and PE pipes based on the case studies.

5.2. Conclusions

In this research, the author used a variety of approaches and case studies to examine the pressure management system and the role of overcut ratio in HDD installation. The analysis reveals that:

- It is difficult to accurately predict the maximum allowable and minimum required pressures and annular pressure during HDD installations due to the uncertainties of the site conditions.
- The Delft solution is the most favorable approach for estimating maximum allowable pressure, however, the results are often underestimated.
- The Herschel–Bulkley model is the most accurate for predicting the annular pressure loss of drilling fluid in HDD. However, the Bingham Plastic model and the Power Law model are preferred due to their convenience and accessibility while still accurate at predicting certain drilling fluid behavior.
- The total pullback force is dependent on the force due to change in direction if the overcut ratio is smaller than 1.5 and dependent on the force due to borehole friction if the overcut ratio is larger than 1.5 for steel pipe; and the total pullback force is dependent on the force due to borehole friction for PE pipes no matter the overcut ratio.
- The pipe diameters have no effect on the percent change in total pullback force for different overcut ratio.
- For sand, the author recommends an overcut ratio of 1.5 for steel pipes in HDD installation; however, for PE pipes, an overcut ratio of 1.3 is adequate for HDD installation.

5.3. Future Research

Currently, there is no method that can accurately predict the maximum allowable pressure in HDD installations. Consequently, more research and field observations are needed for the development of a new approach. For the analysis of overcut ratio in HDD, only Pipeforce method is used and there is no other method to compare it with. Therefore, more methods and field data are needed for validation and a numerical analysis would be beneficial. Moreover, soil properties are not considered in the analysis of overcut ratio and different soil properties have a great effect on the behavior of borehole. As a result, future studies for overcut ratio should incorporate the effect of soil properties in the analysis. Finally, the geometry of borehole and borehole stability are not included in the analysis of overcut ratio and those factors should be considered in the future research as well.

References

Abdollahipour, S., Jeong, D. H. S., Burman, R. R., and Gunsaulis, F. (2011). "Performance assessment of on-grade horizontal directional drilling." Journal of Construction Engineering and Management, 138(3), 458-468.

Alfaro, M. C. and Wong, R.C.K. (2001). "Laboratory studies on fracturing of low-permeability soils." Canadian Geotechnical Journal, 38, 303-315.

Allouche, E. N., Ariaratnam, S. T., and AbouRizk, S. M. (2001). "Applications of horizontal characterization techniques in trenchless construction." Journal of Construction Engineering and Management, 127(6), 476-484.

Allouche, E. N., Ariaratnam, S. T., Lueke, J. S. (2000). "Horizontal Directional Drilling: Profile of an Emerging Industry." Journal of Construction Engineering and Management, 126(1), 68-76.

American Petroleum Institute (API), (2010). "Rheology and Hydraulics of Oil-Well Drilling Fluids." API RP 13D, Washington D.C., US

American Petroleum Institute (API), (2017). "Rheology and Hydraulics of Oil-Well Drilling Fluids." API RP 13D, Washington D.C., US, 32-37.

Arends, G. (2003). "Need and possibilities for a quality push within the technique of horizontal directional drilling." Proc. of 21st No-Dig International Conference and Exhibition 2003 Las Vegas, Nevada, 31 March - 2 April, 16 p.

Ariaratnam, S. T., and Allouche, E. N. (2000). "Suggested practices for installations using horizontal directional drilling." Practice Periodical on Structural Design and Construction, 5(4), 142-149.

Ariaratnam, S. T., Harbin, B. C., and Stauber, R. L. (2007). “Modeling of annular fluid pressures in horizontal boring.” Tunnelling and Underground Space Technology, 22(5), 610-619.

Ariaratnam, S. T., Stauber, R. M., Bell, J., Harbin, B., and Canon, F. (2003). “Predicting and controlling hydraulic fracturing during horizontal directional drilling.” In New Pipeline Technologies, Security, and Safety, 1334-1345.

Ariaratnam, S. T., Stauber, R., and Harbin, B. (2004). “Modeling of Annular Pressures in Horizontal Directional Drilling.” In 2004 International Pipeline Conference, 855-859. American Society of Mechanical Engineers.

ASTM F 1962-11, (2011). “Standard guide for use of maxi-horizontal directional drilling for placement of polyethylene pipe or conduit under obstacles, including river crossings.” ASTM International, West Conshohocken, PA.

Baumert, M. E., Allouche, E. N., and Moore, I. D. (2005). “Drilling fluid considerations in design of engineered horizontal directional drilling installations.” International Journal of Geomechanics, 5(4), 339-349.

Bennett, D. (2009). “Design Issues for HDD Projects.” Trenchless Technology, 2.

Bennett, D., and Wallin, K. (2008). “Step by step evaluation of hydrofracture risks for horizontal directional drilling projects.” In Pipelines 2008: Pipeline Asset Management: Maximizing Performance of our Pipeline Infrastructure, 1-10.

Bingham, E.C. (1922). "Fluidity and Plasticity", McGraw-Hill Book Co., Inc. New York, 463 p.

Blair, G.W.S., Hening, J.C., and Wagstaff, A. (1939). “The flow of cream through narrow glass tubes.” J. Phys. Chem. 43(7), 853-864.

Bleier, R. (1990). “Selecting a drilling fluid.” Journal of Petroleum technology, 42(07), 832-834.

Cai, L., Xu, G., Polak, M. A., and Knight, M. (2017). “Horizontal directional drilling pulling forces prediction methods–A critical review.” Tunnelling and Underground Space Technology, 69, 85-93.

Carlos, A. L., Lillian, D. W., and Patrick, J. C. (2002). “Guidelines for installation of utilities beneath Corps of Engineers levees using horizontal directional drilling.” ERDC/GSL TR-02-9, U.S. Army Corps of Engineers Research and Development Center, Vicksburg, MS.

Carter, J. P., Booker, J. R., and Yeung, S. K. (1986). “Cavity expansion in cohesive frictional soils.” Géotechnique, 36(3), 349–358.

Chehab, A.G. and Moore, I.D. (2012). “Analysis for Long-Term Response of Pipes Installed using horizontal Directional Drilling.” Journal of Geotechnical and Geoenvironmental Engineering, 138(4), 432-440.

Cheng, E., and Polak, M. A. (2007). “Theoretical model for calculating pulling loads for pipes in horizontal directional drilling.” Tunnelling and Underground Space Technology, 22(5-6), 633-643.

Colwell, D. A., and Ariaratnam, S. T. (2003). “Evaluation of high-density polyethylene pipe installed using horizontal directional drilling.” Journal of Construction Engineering and Management, 129(1), 47-55.

Conroy, P. J., Latorre, C. A., and Wakeley, L. D. (2002). “Installation of fiber-optic cables under flood-protection structures using horizontal directional drilling techniques.” US Army Corps of Engineers® Geotechnical Engineering Research Program, ERDC/GSLTR-02-8, 72 p.

Delft Geotechnics. (1997). A report by Department of Foundations and Underground Engineering prepared for O'Donnell Associates, Inc., Sugarland, TX.

Duyvestyn, G. M. (2004). “Field and numerical investigation into pipe bursting and horizontal directional drilling pipeline installation ground movements.” Ph.D. thesis, University of Waterloo, Waterloo, Ontario, Canada. 251 p.

Elwood, D. (2008). “Hydraulic fracture experiments in a frictional material and approximations for maximum allowable mud pressure.” Master’s thesis, Queen’s Univ., Kingston, Canada.

Elwood, E. Y. David, Xia, H., and Moore, I. D. (2007). “Hydraulic fracture experiments in a frictional material and approximations for maximum allowable mud pressure.” Proc. of 60th Canadian Geotechnical Society Annual Conference, Ottawa, Ontario, Canada, 1681-1688.

Frisch-Fay, R., (1962). Flexible Bars. Butterworths, London, UK, pp. 73–80.

Hair III, C. W. (1995). “Site Investigation Requirements for Large Diameter HDD Projects.” In New Advances in Trenchless Technology: An Advanced Technical Seminar.

Hashash, Y., Javier, J., Petersen, T., and Osborne, E. (2011). “Evaluation of Horizontal Directional Drilling (HDD).” Civil Engineering Studies, Illinois Center for Transportation Series IDOT Report, FHWA-ICT-11-095, UILU-ENG-2011-2021, 51 p.

Herschel, W.H. and Bulkley, R. (1926), "Konsistenzmessungen von Gummi-Benzollösungen." Kolloid Zeitschrift, 39, 291–300, doi:10.1007/BF01432034.

Huey D.P., Hair J.D., McLeod K.B., (1996). “Installation loading and stress analysis involved with pipelines installed in horizontal directional drilling.” In: Proc. of No-Dig 96, New Orleans, USA, 37–60.

Kelessidis, V., Maglione, R., Tsamantaki, C. and Aspirtakis, Y. (2006). "Optimal determination of rheological parameters for Herschel–Bulkley drilling fluids and impact on pressure drop, velocity profiles and penetration rates during drilling." Journal of Petroleum Science and Engineering 53(3), 203-224.

Kennedy, M. J., Skinner, G. D., and Moore, I. D. (2004a). “Elastic calculations of limiting mud pressures to control hydrofracturing during HDD.” Proc., No-Dig 2004.

Kennedy, M. J., Skinner, G. D., and Moore, I. D. (2004b). “Limiting mud pressures to control hydrofracturing during HDD in an elastoplastic soil.” In Proc., 2004 Canadian Geotechnical Society Conf.

Kennedy, M. J., Skinner, G. D., and Moore, I. D. (2006). “Development of tensile hoop stress during horizontal directional drilling though sand.” ASCE International Journal of Geomechanics, 6(5), 367-372.

Keulen, B. (2001). “Maximum allowable pressures during horizontal directional drillings focused on sand.” Ph.D. thesis, Delft Univ. of Technology, Delft, Netherlands.

Kirby, M., Kramer, S. R., Pittard, G. T., and Mamoun, M. (1996). ‘‘Design guidelines and procedures for guided horizontal drilling.’’ Proc., 1996 Int. No-Dig Conf. and Exhibition.

Langlinais, J.P., Bourgoyne, A. T., Holden, W. R. (1983): Frictional Pressure Losses for the Flow of Drilling Mud and Mud/gas Mixtures, paper SPE 11993 presented at the Annual Technical Conference, San Francisco, CA, October 5-8.

Lu, J., Zhang, H., and Ma, Q. (2012). “Drilling fluid pressure calculation in horizontal directional drilling.” Proc. of International Conference on Pipelines and Trenchless Technology October 19-22, Wuhan, China, 1870-1879.

Lueke, J. S., and Ariaratnam, S. T. (2005). “Surface heave mechanisms in horizontal directional drilling.” Journal of Construction Engineering and Management, 131(5), 540-547.

Luger, H. J., and Hergarden, H. J. A. M. (1988). “Directional drilling in soft soil: influence of mud pressures.” Proc. of 3rd Int. Conf. on Trenchless Technology—No-Dig Conf., International Society for Transgenic Technologies, London.

Marken, C.D, He, X., Saasen A. (1992). “The Influence of drilling conditions on annular pressure losses.” Proc. of SEP 67th Annual Technical Conference and Exhibition, Washington D.C., October 4-7, 553-567.

Mesri, G. and Hayat, T.M. (1993). “The coefficient of earth pressure at rest.” Canadian Geotech. Journal, 30(4), 647-666.

Mo, P. Q. and Yu, H. S. (2016). “Undrained cavity expansion analysis with a unified state parameter model for clay and sand.” Géotechnique, 67(6), 503-515.

Moore, I.D. (2005). Analysis of ground fracture due to excessive mud pressure, Proc. of 2005 No-Dig Conference, New Orleans, Florida, Paper C-1-03-1.

Murdoch, L.C. (1993a). “Hydraulic fracturing of soil during laboratory experiments: methods and observations.” Geotechnique, 43(2), 255-265.

Murdoch, L.C. (1993b). “Hydraulic fracturing of soil during laboratory experiments: propagation.” Geotechnique, 43(2), 266-276.

Murdoch, L.C. (1993c). “Hydraulic fracturing of soil during laboratory experiments: theoretical analysis.” Geotechnique, 1993c, 43(2), 276-287.

Murray, C., Bayat, A., Osbak, M., (2014). Elevated annular pressure risk in horizontal directional drilling. In: Proc., 2014 NASTT Conf., Orlando, MA-T6-03.

Ngan, K.G. (2015). “Predicting Soil Expansion Force in Static Pipe Bursting Using Cavity Expansion Solutions and Numerical Modeling.” Master’s of Science Thesis, University of Alberta, Edmonton, Alberta, Canada. 101 p.

Ofei, T.N. (2016). “Effect of Yield Power Law Fluid Rheological Properties on Cuttings Transport in Eccentric Horizontal Narrow Annulus,” Journal of Fluids, 2016, 10 p. doi:10.1155/2016/4931426

Okafor, M.N. and Evers, J.F. (1992). “Experimental comparison of rheology models for drilling fluids.” SPE Western Regional Meeting, Bakersfield, California, March 30-April 1, 575-581.

Osbak, M. (2011). “Theory and application of annular pressure management.” Proc., No-Dig Conf., North American Society for Trenchless Technology (NASTT), Cleveland.

Polak, M. A., and Lasheen, A. (2001). “Mechanical modelling for pipes in horizontal directional drilling.” Tunnelling and underground space technology, 16, 47-55.

Polak, M. A., and Chu, D. (2005). “Pulling loads for polyethylene pipes in horizontal directional drilling: theoretical modeling and parametric study.” Journal of infrastructure systems, 11(2), 142-150.

Polak, M. A., Duyvestyn, G., and Knight, M. (2004). “Experimental strain analysis for polyethylene pipes installed by horizontal directional drilling.” Tunnelling and underground space technology, 19(2), 205-216.

Popelar, C. H., Kuhlman, C. J., and Mamoun, M. M. (1997). ‘‘Guidelines for installing PE pipe using HDD techniques.’’ Pipeline and Gas In- dustry Mag., December, 43–49.

Rostami, A. (2017). “Prediction and Evaluation of Annular Pressure in Horizontal Directional Drilling.” Ph.D. thesis, University of Alberta, Alberta, Canada.

Rostami, A., Yi, Y., and Bayat, A. (2016). “Estimation of Maximum Annular Pressure during HDD in Noncohesive Soils.” International Journal of Geomechanics, 17(4), 06016029.

Rostami, A., Yi, Y., Bayat, A., and Osbak, M. (2016). “Annular fluid pressure estimation during pilot boring in horizontal directional drilling using the Bingham plastic flow model.” International Journal of Petroleum Engineering, 2(2), 79-90.

Royal, A. C. D., Riggall, T. J., and Chapman, D. N. (2010). "Analysis of steering in horizontal directional drilling installations using down-hole motors." Tunnelling and Underground Space Technology, 25(6), 754-765.

Royal, A. C., Polak, M. A., Rogers, C. D. F., and Chapman, D. N. (2010). "Pull-in force predictions for horizontal directional drilling." Proceedings of the Institution of Civil Engineers-Geotechnical Engineering, 163(4), 197-208.

Shu, B., Ma, B.S., (2015). "Study of ground collapse induced by large diameter horizontal directional drilling in sand layer using numerical modeling." Can. Geotech. J. 52(10): 1562-1574, https://doi.org/10.1139/cgj-2014-0388

Shu, B., Ma, B.S., Lan, H.T., (2015). "Cuttings transport mechanism in a large-diameter HDD borehole." J. Pipeline Syst. Eng. Pract., 6(4): 0401401-7

Simon, K. (2004). "The role of different rheological models in accuracy of pressure loss prediction." Rudarsko-Geolosko-Naftni Zbornik, 16(1), 85.

Staheli, K., Bennett, D., O'Donnell, H. W., and Hurley, T. J. (1998). "Installation of Pipelines beneath Levees Using Horizontal Directional Drilling" USAE Waterways Experiment Station, Technical Report CPAR-GL-98-1, April, 1998

Staheli, K., Christopher, G. P., and Wetter, L. (2010). "Effectiveness of hydrofracture prediction for HDD design." North American Society for Trenchless Technology (NASTT), Chicago, IL.

Subramanian, R. and Azar, J.J. (2000). "Experimental study on friction pressure drop for NonNewtonian drilling fluids in pipe and annular flow." Proc. Of SPE International Oil & Gas Conference and Exhibition in China, Beijing, China, 7-10 November, 11 p.

Tanzi, D., Andreasen, G.C., Jr. (2011). “Contingency planning for high-risk HDD construction.” North American Society for Trenchless Technology (NASTT), Washington, D.C.

Vajargah, A.K. and van Oort,E. (2015). “Determination of drilling fluid rheology under downhole conditions by using real-time distributed pressure data.” Journal of Natural Gas Science and Engineering, 24, 400-411.

Van, B.G., Hergarden, H.J.A.M. (1997). “Installation of pipelines beneath levees using horizontal directional drilling.” Delft Geotechnics, SO-59407-701/2, pp. 1–16.

Verruijt, A. (1993). Grondmechanica, Delftse Uitgevers Maatschappij, Delft, Netherlands.

Verwey, K. (2013). “Real time data acquisition and prediction model comparison using maxi directional drills.” Masters’ of Science Thesis, University of Waterloo, 36 p.

Vesic, A. S. (1972). “Expansion of cavities in infinite soil mass.” J. Soil Mech. Found. Div., 98(3), 265–290.

Viloria Ochoa, M. (2006). “Analysis of drilling fluid rheology and tool joint effect to reduce errors in hydraulics calculations” (Doctoral dissertation, Texas A&M University).

Wang, X. and Sterling, R.L. (2007). “Stability analysis of a borehole wall during horizontal directional drilling.” Tunnelling and Underground Space Technology, 22, 620–632

Wang, X., Sterling, R.L. (2006). Finite element analysis of the instability of borehole wall during horizontal directional drilling, 2006 No Dig Conference Brisbane, Australia, 49: 1-16.

Xia, A. (2009). “Investigation of maximum mud pressure within sand and clay during horizontal directional drilling.” Ph.D. thesis, Queen’s Univ., Kingston, Canada.

Xia, H., and Moore, I. D. (2006). “Estimation of maximum mud pressure in purely cohesive material during directional drilling.” Int. J. Geomech. Geoeng. 1(1), 3–11.

Xia, H., and Moore, I. D. (2007). “Discussion of limiting mud pressure during directional drilling in clays.” Proc., Geo2007, Canadian Geotechnical Society, Richmond, BC, Canada.

Yan, X., Ariaratnam, S. T., Dong, S., and Zeng, C. (2018). “Horizontal directional drilling: State-of-the-art review of theory and applications.” Tunnelling and Underground Space Technology, 72, 162-173.

Yan, X., Ma, B., Zeng, C., and Liu, Y. (2016). “Analysis of formation fracturing for the Maxi-HDD Qin River crossing project in China.” Tunnelling and Underground Space Technology, Volume 53, 2016, Pages 1-12, ISSN 0886-7798, https://doi.org/10.1016/j.tust.2015.11.018.

Yan, X., Sayem, S., Allouche, E., and Alam, S. (2015). “Experimental Examination of the Mathematical Model for Predicting the Borehole Pressure during Horizontal Directional Drilling.” In Pipelines 2015, 109-122.

Yu, H. S., and Houlsby, G. T. (1991). “Finite cavity expansion in dilatant soil: Loading analysis.” Géotechnique, 41(2), 173–183.

Zamora, M., Jefferson, D.T., and Powell, J.W. (1993). “Hole-Cleaning Study of Polymer-Based Drilling Fluids”. Proc. Of 68th Annual Technical Conference and Exhibition of the Society of Petroleum Engineers Houston, Texas, 3-6 October, 151-162.